sustainability

MDPI

Review

Aspects of Spodumene Lithium Extraction Techniques

Nagaraj Nandihalli [1,*], Rajiv K. Chouhan [2], Rambabu Kuchi [1] and Ihor Z. Hlova [1,*]

[1] Critical Materials Innovation Hub, Ames National Laboratory, U.S. Department of Energy, Iowa State University, Ames, IA 50011, USA
[2] Ames National Laboratory, U.S. Department of Energy, Iowa State University, Ames, IA 50011, USA
* Correspondence: nagaraj.nandi001@umb.edu (N.N.); ihlova@ameslab.gov (I.Z.H.)

Abstract: Lithium (Li), a leading cathode material in rechargeable Li-ion batteries, is vital to modern energy storage technology, establishing it as one of the most impactful and strategical elements. Given the surge in the electric car market, it is crucial to improve lithium recovery from its rich mineral deposits using the most effective extraction technique. In recent years, both industry and academia have shown significant interest in Li recovery from various Li-bearing minerals. Of these, only extraction from spodumene has established a reliable industrial production of Li salts. The current approaches for cracking of the naturally occurring, stable α-spodumene structure into a more open structure—β-spodumene—involve the so-called decrepitation process that takes place at extreme temperatures of ~1100 °C. This conversion is necessary, as β-spodumene is more susceptible to chemical attacks facilitating Li extraction. In the last several decades, many techniques have been demonstrated and patented to process hard-rock mineral spodumene. The objective of this review is to present a thorough analysis of significant findings and the enhancement of process flowsheets over time that can be useful for both research endeavors and industrial process improvements. The review focuses on the following techniques: acid methods, alkali methods, carbonate roasting/autoclaving methods, sulfuric acid roasting/autoclaving methods, chlorinating methods, and mechanochemical activation. Recently, microwaves (MWs), as an energy source, have been employed to transform α-spodumene into β-spodumene. Considering its energy-efficient and short-duration aspects, the review discusses the interaction mechanism of MWs with solids, MW-assisted decrepitation, and Li extraction efficiencies. Finally, the merits and/or disadvantages, challenges, and prospects of the processes are summarized.

Keywords: spodumene; lithium extraction efficiency; decrepitation; calcination; microwave-assisted decrepitation

check for updates

Citation: Nandihalli, N.; Chouhan, R.K.; Kuchi, R.; Hlova, I.Z. Aspects of Spodumene Lithium Extraction Techniques. *Sustainability* **2024**, *16*, 8513. https://doi.org/10.3390/su16198513

Academic Editor: Yasukazu Kobayashi

Received: 28 August 2024
Revised: 21 September 2024
Accepted: 25 September 2024
Published: 30 September 2024

Copyright: © 2024 by the authors. Licensee MDPI, Basel, Switzerland. This article is an open access article distributed under the terms and conditions of the Creative Commons Attribution (CC BY) license (https://creativecommons.org/licenses/by/4.0/).

1. Introduction

Lithium is ranked as the 25th most prevalent element in the earth's crust, with an average concentration of 20 mg/kg. Due to its strong reactivity, pure elemental lithium is not found in nature. Li is utilized as an exceptional cathode material (e.g., $LiFePO_4$, $LiCoO_2$, $LiMn_2O_4$, and $LiNi_xCo_yMnZO_2$) in rechargeable Li-ion batteries (LiBs) due to its unmatched energy density per unit weight and elevated electrochemical potential of 3.045 V [1]. It has the highest specific heat capacity, is the lightest of all solid elements (with a density of 0.534 g/cm^3 at 20 °C), and has the smallest ionic radius of all the alkali metals [2]. Such features provide batteries with high gravimetric and volumetric energy densities [3]. The growing utilization of LiBs in various products, such as mobile phones, laptops, health-monitoring sensors, camcorders, tracking systems, and military equipment, necessitates a substantial reliance on Li resources and accessibility. According to an International Energy Agency (IEA) report, in 2022, the resurgence in passenger and cargo transportation activity after the COVID-19 pandemic resulted in a 3% increase in transport CO_2 emissions over the previous year. From 1990 to 2022, transport emissions increased at an annual average rate of 1.7%, faster than any other end-use sector, with the exception of

industry (which expanded at ~1.7%). To achieve Net-Zero Emissions (NZE) by 2050, CO_2 emissions from the transportation sector must decrease by at least 3% per year until 2030. As a result, governments around the world are aggressively encouraging the electrification of the transportation industry. Reducing carbon emissions by developing zero-emission buses, cars, and trucks is also a vital step toward combating global warming. The rapid deployment of green low-carbon hybrid electric vehicles (HEVs) and fully electric vehicles (EVs) [4] technology has ushered a critical role of LIBs in modern energy storage solutions into the spotlight. In addition to energy storage, lithium chloride, a lithium derivative, is used in high-temperature processes, such as ceramic and glass manufacturing [2,5,6]. In 2025, global demand for Li is predicted to exceed 1.4 million metric tons of lithium carbonate equivalent, a 53% increase over 2023. An increase in battery demand for EVs will be a prime factor in Li usage during the next decade (M. Jaganmohan of Statista+). The role of Li in the fulfillment of the global energy storage and its utilization demand is vital for the future energy age.

A significant percentage of the present Li supply is derived from the processing of Li-containing brines, which originate in desiccated salt lakes known as salars. The largest salars are only found in South America. Chile, which extracts Li from brines, is one of the world's top-three Li producers. The Li concentration in most brines ranges from 200 to 700 ppm (1000 ppm in some brines [7]), which is insufficient to use commercially; thus, preconcentration is required. The lime soda evaporation process is the primary method for recovering Li from brines and consists of several phases, beginning with concentration by evaporation, followed by impurity elimination and precipitation by carbonation. Li production from brine is often 30–50% less expensive than from hard-rock sources [8].

The present evaporitic approach for extracting Li from continental brine deposits concentrates the brine through open-air evaporation. However, concerns regarding the process's overall sustainability are raised by the significant amounts of water lost through evaporation—between 100 and 800 m^3/tons of lithium carbonate, depending on the deposit. Moreover, brine concentration is a naturally slow process that takes 10–24 months; thus, it is not sensitive to fluctuations in demand over the near term [9]. Furthermore, the processing of these minerals raises a variety of serious environmental challenges.

Pegmatite ores are the second most important source of Li after salars [10]. Spodumene ($LiAlSi_2O_6$), lepidolite ($K(Li,Al,Rb)_2(Al,Si)_4O_{10}(F,OH)_2$), petalite, and zinnwaldite are minerals found in pegmatites. Currently, these Li-containing ores account for more than half of the Li reserves, with spodumene-enriched ores dominating [10,11]. The amount of lithium oxide (Li_2O) in spodumene corresponds to about 8%, which is about 4% Li. Spodumene typically occurs alongside other lithium aluminosilicates, such as eucryptit ($LiAlSiO_4$) and/or petalite ($LiAlSi_4O_{10}$). Other important Li-bearing minerals are listed in Table 1. Li extraction from ores and minerals utilizes roasting, followed by leaching [12,13]. Pegmatites are more expensive to process than brines because of the heating and dissolution stages necessary. The higher metal concentration in pegmatites, however, somewhat offsets the expenses.

Table 1. Major Li-bearing minerals [14].

Mineral	Formula	Theoretical Li Content (%)
Amblygonite	$(Li,Na)AlPO_4$ (OH,F)	4.73
Bikitaite	$LiAlSi_2O_6 \cdot H_2O$	3.40
Elbaite	$Na(Li_{1.5}Al_{1.5})Al_6Si_6B_3O_{27}(OH)_4$	1.11
Eucryptite	$LiAlSiO_4$	5.51
Hectorite	$Na_{0.3}(Mg,Li)_3Si_4O_{10}(OH)_2$	~1.93

Table 1. *Cont.*

Mineral	Formula	Theoretical Li Content (%)
Jadarite	$LiNaAlSiB_2O_7(OH)$	2.85
Lepidolite	$KLi_2AlSi_3O_{10}(OH,F)_2$	~3.84
Lithiophylite	$LiMnPO_4$	4.43
Montebrasite	$LiAl(PO_4)(OH)$	1 to 4
Petalite	$LiAlSi_4O_{10}$	2.27
Spodumene	$LiAlSi_2O_6$	3.73
Triphylite	$LiFePO_4$	4.40
Zabuyelite	Li_2CO_3	18.79
Zinnwaldite	$KLiFeAl_2Si_3O_{10}(F,OH)_2$	1.59

The most commonly found natural form of spodumene is α-spodumene (monoclinic structure with a density of 3.184 g/cm^3), which can be transformed to β-spodumene (tetragonal structure [15] with a density of 2.374 g/cm^3) by heating above 900 °C. A third spodumene polymorph, γ-spodumene or virgilite (hexagonal structure with a density of 2.399 g/cm^3) [16], is thought to form at a lower temperature and then convert to β-spodumene at higher temperatures (Figure 1) [17]. The γ-spodumene phase is metastable with regard to β-spodumene and is difficult to distinguish from β-spodumene due to X-ray diffraction pattern similarities. The relationships between the specific heat capacities (C_p) of the three phases have been computed with respect to temperature, as [18]:

$$C_p(T) = 354.715 - 3375.72T^{-0.5}\ \mathrm{Jmol^{-1}K^{-1}} \quad (1)$$

$$C_p(T) = 362.8 - 0.003684T - 3435.0T^{-0.5}\ \mathrm{Jmol^{-1}K^{-1}} \quad (2)$$

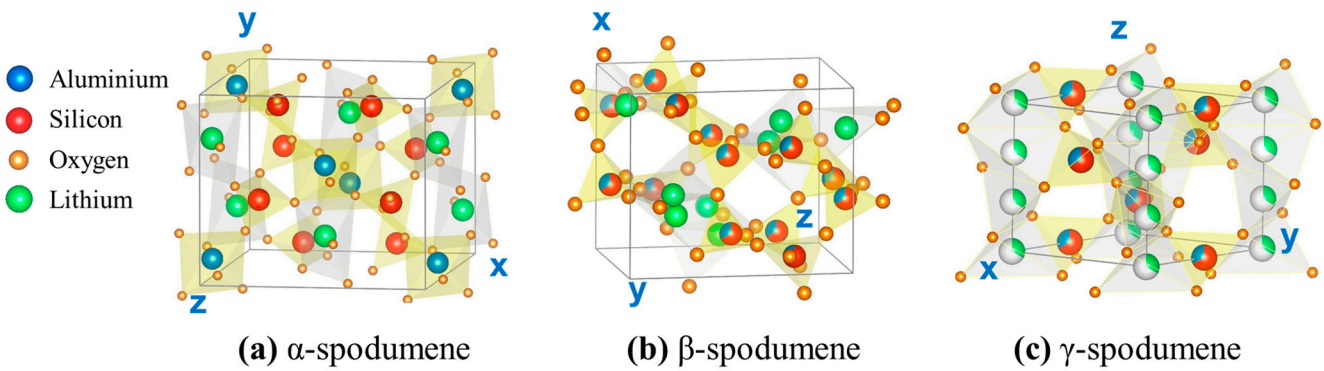

Figure 1. Crystal structures of spodumene polymorphs: (**a**) α-spodumene, (**b**) β-spodumene, and (**c**) γ-spodumene.

The Cp (300 K) of α-, β-, and γ-spodumene are 158.93, 162.77, and 162.77 J/K-mol, respectively.

A heat treatment (1050–1100 °C) [12] is required to convert monoclinic α-spodumene to tetragonal β-spodumene in order to offer a pathway for Li liberation with volume expansion, due to the drop in specific gravity (3.2 g/cm^3 to 2.4 g/cm^3) [19], making it more accessible to extraction reagents. According to thermodynamic data, it is evident that the transition from α- to β-spodumene is not thermodynamically favorable under ordinary ambient temperature settings. However, this change can be accomplished by increasing the temperature:

$$\beta - \text{spodumene} \xleftarrow{\Delta G_{298\ \mathrm{K}=\ 4.63\ \mathrm{kcal}}} \alpha - \text{spodume} \xrightarrow{\Delta G_{1073\ \mathrm{K}=-0.45\ \mathrm{kcal}}} \beta - \text{spodumene} \quad (3)$$

The Gibbs free energy change vs. temperature information suggests the possibility of a phase conversion at ≥800 °C, although studies in this direction have revealed that a higher temperature is required to convert the α-phase to the β-phase, which was validated by XRD analysis [20].

Roasting and calcination are the two common thermal treatments to transform (decrepitate) α-spodumene to β-spodumene [21–23]. The process of roasting occurs in the presence of air, facilitating the chemical reaction between oxygen and minerals to produce oxides. Various additives, such as sulfate, chloride, and carbonate, can be utilized to facilitate the processing of Li into soluble sulfate, chloride, or bicarbonate complexes. Calcination is commonly conducted at elevated temperatures, usually below 1000 °C, under conditions of oxygen deprivation and frequently in the presence of additives: lime or limestone. Calcination is also used to improve spodumene beneficiation since the final product, β-spodumene, is chalky, soft, and easy for grinding compared to gangue minerals, such as quartz and feldspar. As a result, grinding the calcination product followed by size separation has been proposed as a method for enriching spodumene [24]. Current Li mining, beneficiation, and extraction practices are ecologically and socio-environmentally unfriendly and unsustainable [25,26]. Tailings from Li mining contain heavy metals that can slowly seep into the soil, groundwater, or surface water. The same holds true for discarded batteries, unless they are recycled. Despite notable progress in the application of Li, the development of alternate Li extraction technologies for hard-rock minerals has not kept pace. Moreover, there exists a significant potential to improve current techniques by employing novel unconventional technologies, such as microwave decrepitation or mechanochemical activation.

The chemical and mineral compositions of resources should be determined before assessing them for metallurgical beneficiation and subsequent extraction operations. This is critical in selecting various units of operation and understanding the material's response and behavior throughout processing and beneficiation [27]. Sample preparation is one of the most important phases in mineral chemical analysis, and it can be time-consuming and prone to errors, as well as the use of harsh reagents, which results in the chemical residue formation [28–31]. The chemical analysis of spodumene is typically accomplished by combining fusion followed by acid digestion. Inductively coupled plasma spectroscopy (ICP) [32], ion-selective electrodes [33], and X-ray fluorescence (XRF) [34] are commonly used to determine the chemical composition of a material. X-ray diffraction (XRD) [35] and quantitative assessment of minerals by scanning electron microscopy (QEMSCAN) [36], on the other hand, have proved useful in establishing the detailed mineralogical composition of many materials, including mineral liberation and association relationships. Volpi et al. developed a MW-assisted procedure for chemical analysis of α-spodumene, aiming to determine the contents of Li and other metals of interest [37]. Instead of using conventional high volumes/concentrations of HF to break the crystalline structure, they used an acid mixture composed of sulfuric and phosphoric acids and diluted hydrofluoric acid solution. The sample heating was performed in 60 min at a maximum temperature of 230 °C (with 1800 W maximum microwave power) using closed vessels for digestion of α-spodumene. All elements were determined by inductively coupled plasma optical emission spectrometry (ICP-OES).

The subsequent sections review the recent and traditional Li recovery techniques, encompassing acid methods (Section 2.1), chlorination methods (Section 2.2), carbonate roasting and autoclaving methods (Section 2.3), alkali methods (Section 2.4), sulfate roasting (Section 2.5), MW-assisted decrepitation and Li extraction (Section 2.6), and mechanical activation (Section 2.7). A short discussion on recycling spent LIBs is included because recycling promotes the development of a circular economy, in which effective usage of natural resources is emphasized and waste output is reduced to support the development and sustenance of cleaner Li-based energy storage systems (Section 3). The review concludes with a concise summary, challenges, and outlook. The factors that may have an impact on

the long-term viability of Li mining, the issues with present recovery technologies, and prospective solutions to problems are all examined.

2. Lithium Recovery from Spodumene

Several methods have been devised to extract Li from its minerals, including physical beneficiation, followed by chemical treatment. Complex ores undergo physical beneficiation processes, such as size reduction, froth flotation, and magnetic separation, to enrich their metallic values [12,19,38,39]. The resulting concentration is then utilized to recover Li via a combined heat treatment and chemical processing methods. Froth flotation is the most often used method for spodumene and other ore beneficiation. It is a process that uses mineral surface characteristics to concentrate Li minerals from pegmatite ores [40]. Reverse and direct flotation techniques have been employed to concentrate Li minerals from pegmatite ores. In reverse flotation, gangue minerals are floated with cationic collectors to produce spodumene concentrate, while direct flotation uses anionic collectors to reject gangue minerals. Flotation can selectively recover minerals depending on characteristics such as mineral surface chemistry, collector type and concentration, pulp pH, pre-treatment procedures, surface characteristics, and slime presence [40–42]. Magnetic separation can be employed before or after flotation to separate iron-bearing particles and prepare the concentrate for further processing.

There are two types of Li extraction operations from spodumene: direct methods (without decrepitation pre-treatment) and indirect methods (after decrepitating α- to β-spodumene). The subsequent sections will provide a comprehensive discussion on the methodologies employed for the recovery of Li from both α-spodumene and β-spodumene. The documented methods for recovering Li from spodumene are essentially classified into five categories: (1) acid methods, (2) alkali methods, (3) carbonate roasting/autoclaving methods, (4) sulfate roasting/autoclaving methods, and (5) chlorinating methods. Recent research shows that microwave-assisted heating can be used to achieve the α–β–γ-phase change of spodumene, as discussed in Section 2.6, and mechanochemical activation allows to process α-spodumene directly, as described in Section 2.7.

2.1. Acid Methods

2.1.1. Sulfuric Acid

Currently, this process continues to maintain its dominance in the sector of Li extraction from spodumene. The utilization of sulfuric acid (H_2SO_4) as an acid technique has only been established for β-spodumene due to the low reactivity observed between α-spodumene and H_2SO_4. The sulfuric acid method includes the following steps: calcination, acid roasting, leaching, purification, evaporation, Li precipitation, and anhydrous sodium sulfate concentration and crystallization. In this process, pulverized β-spodumene is roasted with concentrated H_2SO_4 at a temperature of 250 °C (reaction represented by Equation (3)). According to the reports, the crystal structure of β-spodumene remains intact during the roasting process. However, the original location of Li^+ ions inside the crystal lattice is occupied by H^+ ions, leading to the formation of $H_2O{\cdot}Al_2O_3{\cdot}4SiO_2$ [43]. After being roasted with H_2SO_4, the calcine was leached by water to convert to dissolve the sulfates (Equation (5)), and then neutralized by adding calcium carbonate ($CaCO_3$) to eliminate leftover H_2SO_4 and some impurities. The crude Li_2SO_4 solution that resulted was then filtered to remove Ca, Mg, Al, and Fe. Following that, as shown in Equation (6), the majority of the Li ions are precipitated after addition of sodium carbonate (Na_2CO_3) to the concentrated solution, followed by formation of sodium sulfate (Na_2SO_4) and leftover Li recoveries. Figure 2 depicts a Li extraction from β-spodumene using H_2SO_4, followed by purification and recovery processes.

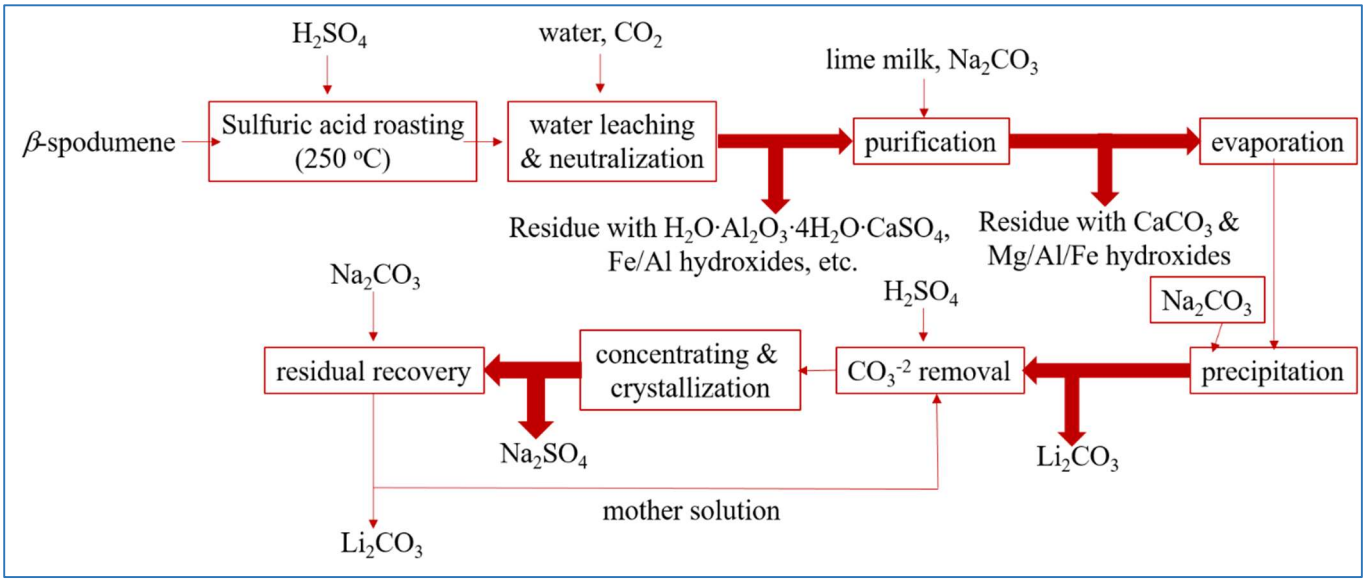

Figure 2. The recovery procedure of Li from β-spodumene by the utilization of the sulfuric acid roast method. Adapted with permission from [21].

For the roasting and leaching conditions, the sulfuric acid roast process was thoroughly investigated and optimized [44]. At 140% of stoichiometric excess, 93% H_2SO_4 was utilized, with a roasting temperature of 250 °C and a roasting time of 30 min. After 15 min of water leaching at room temperature (RT) and a liquid-to-solid (L/S) ratio of 1.85, a Li extraction yield of 96.9% was achieved. Yet, there are several disadvantages associated with this process. Roasting with concentrated H_2SO_4 increases equipment wear and costs and produces environmentally harmful acid waste. When roasting is completed in a rotary kiln, optimal temperature control and energy recovery are difficult. Furthermore, the precipitated Fe and Al impurities are relatively abundant and have a tendency to capture Li, resulting in lower yields. Because of these limitations, researchers have been actively exploring other methods that could be used as an alternative to the sulfuric acid roast process.

$$\beta - Li_2O{\cdot}Al_2O_3{\cdot}4SiO_2(s) + H_2SO_4(conc) \rightarrow H_2O{\cdot}Al_2O_3{\cdot}4SiO_2(s) + Li_2SO_4(s),\ \Delta G^o_{250\ ^\circ C} = -151.38\ kJ/mol \quad (4)$$

$$Li_2SO_4(s) \rightarrow \overrightarrow{H_2O} = Li_2SO_4(aq),\ \Delta G^o_{25\ ^\circ C} = -10.07\ kJ/mol \quad (5)$$

$$Li_2SO_4(aq) + Na_2CO_3(aq) \rightarrow Li_2CO_3(s) + Na_2SO_4(aq), \Delta G^o_{25\ ^\circ C} = -17.54\ kJ/mol \quad (6)$$

2.1.2. Hydrofluoric Acid (HF)

Many experimental studies have indicated that HF acid dissolves both α-spodumene and β-spodumene phases [11,45]. The breakdown of β-spodumene in HF can be represented by the following reaction [46]:

$$LiAlSi_2O_6(s) + 19HF(aq) \rightarrow LiF(aq) + H_3AlF_6(aq) + 2H_2SiF_6(aq) + H_2O \quad (7)$$

According to Kuang et al. [45], at ~225 °C, HF produced by fluorite and sulfuric acid continues to react with α-spodumene, producing intermediates. HF initially breaks the basic bonds of Li-O, Al-O, Si-O, and Al-O-Si inside spodumene, resulting in the formation of Li_3AlF_6, AlF_3, SiF_4, and other compounds. These intermediates then react with sulfuric acid, producing Li_2SO_4 and $Al_2(SO_4)_3$. Li^+, Al^{3+}, and other metal ions are soluble in water and can be recovered from aqueous extracts. The process of the Li extraction reaction is delineated as follows:

HF generation:

$$CaF_2(s) + H_2SO_4(l) \rightarrow CaSO_4(s) + 2HF(g)\uparrow \quad (8)$$

Transformation of corroded residue by sulfuric acid:

$$\begin{aligned} 2Li_3AlF_6 + 6H_2SO_4 &\rightarrow 3Li_2SO_4 + Al_2(SO_4)_3 + 12HF\uparrow \\ 2AlF_3 + 3H_2SO_4 &\rightarrow Al_2(SO_4)_3 + 6HF\uparrow \end{aligned} \quad (9)$$

Guo et al. [47] suggested an approach for accelerating Li leaching from α-spodumene utilizing the mixed acid HF/H_2SO_4 as a lixiviant without a phase conversion (Figure 3c). Under far more moderate conditions (at 100 °C), more Li (96%) may be transferred into lixivium. Prior to conducting dissolution experiments, the α-spodumene ore (Greenbushes, Australia) was pulverized in a planetary ball mill machine and sieved to a particle size of <75 µm. Concentrated sulfuric acid (18.2 M H_2SO_4, 98% (wt%)) and hydrofluoric acid (22.5 M HF, 40% (wt%)) were employed.

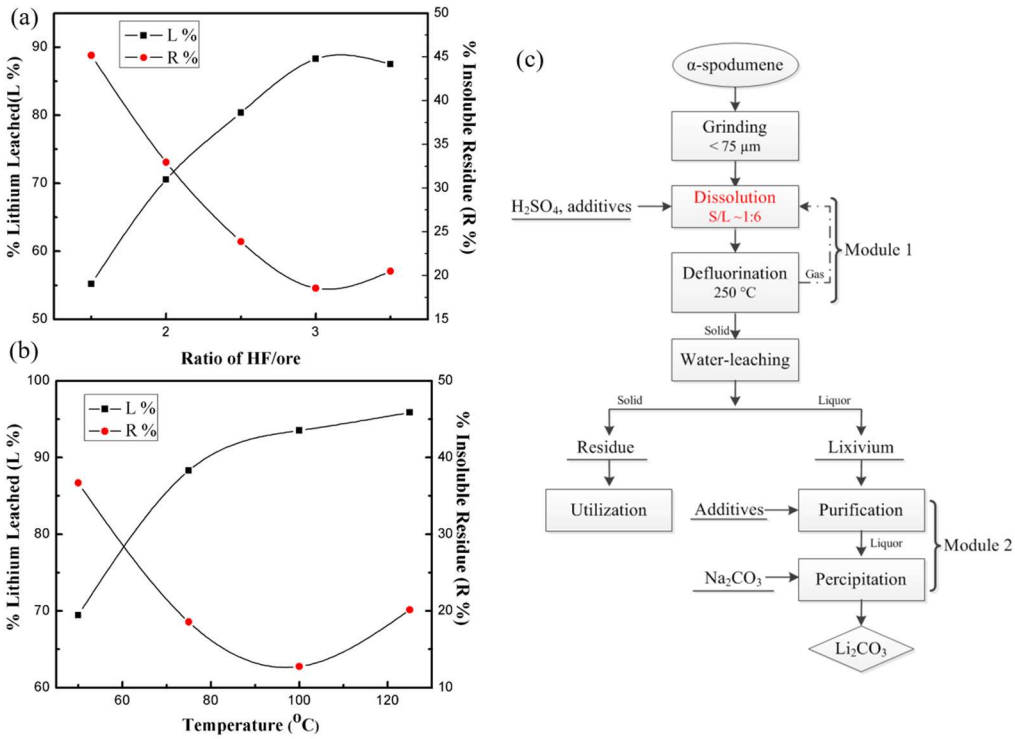

Figure 3. (**a**) Effect of different mass ratios of HF/ore on the dissolution process (75 °C, ore/H_2SO_4 1:2.5, 150 rpm, 3 h). (**b**) Effects of temperature on the dissolution process (ore/HF/H_2SO_4 1:3:2.5, 150 rpm, 3 h). (**c**) Flowchart of the fluorine sulfuric acid technique for extracting Li from α-spodumene [47].

The dissolution studies were carried out in a 100 mL Teflon crucible fitted with a magnetic stirring device and held in an oil bath at a predetermined temperature. In a reactor, 10 g of ore, deionized water, and 1:1 H_2SO_4 were mixed and continually agitated. Once the desired temperature (50 to 125 °C) was reached, HF was added, and stirring at 150 rpm was maintained for a set amount of time. Water leaching was then performed at 50 °C with an ore/water ratio of 1:8 (g/mL) and agitated at 150 rpm for 30 min. After cooling the slurry to RT, the liquid and solids were separated by filtration and analyzed. Experiments conducted with various ore-to-HF ratios demonstrated that the leaching efficiency of lithium (L%) increased as the ratio of HF to ore was raised (Figure 3a). Approximately 90% of the Li was leached from the ore when the ratio of ore to HF was 1:3. And yet, the increase in the ore-to-HF ratio to 1:3.5 resulted in a decline in the L% and a rise in the percentage of

insoluble residues (R%). Experiments were carried out at various dissolution temperatures from 50 to 125 °C, suggesting that Li leaching accelerated with the increasing temperature (Figure 3b).

Experiments on extracting Li from β-spodumene with HF acid leaching [11] revealed that the most favorable conditions for achieving a Li extraction rate exceeding 90% were as follows: a solid-to-liquid ratio of 1.82% (w/v), a leaching temperature of 75 °C, an HF concentration of 7% (v/v), a stirring speed of 330 rpm, and a reaction time of 10 min. The compounds Na_3AlF_6 and Na_2SiF_6 were produced as byproducts, with a recovery rate of 92%. The dissolved Li ions can be effectively separated by precipitating them as lithium carbonate (Li_2CO_3), resulting in recovery rates of ~90%. In this investigation, the α-phase (Las Cuevas, Argentina) was calcined at 1100 °C to obtain the β-phase.

Apart from the above conditions, the effect of particle size on Li extraction efficiency was also ascertained. The data shown in Figure 4a demonstrate a clear inverse relationship between particle size and Li extraction efficiency. The observed phenomenon can be ascribed to an increase in the interfacial area between the mineral and HF when the particle size decreases. When the leaching temperature was raised from 10 to 75 °C, the extraction efficiency rose significantly. When the reaction temperature was 50 °C, the extraction efficiency reached 98%. However, it was noticed that increasing the temperature did not result in a significant increase in the extraction efficiency (Figure 4b). Experiments were carried out to explore the influence of the reaction time on Li extraction under conditions of a 1.82% (w/v) solid-to-liquid ratio, 7% (v/v) HF concentration, 25 °C temperature, and 330 rpm stirring speed. The leaching time had a significant impact on Li extraction. The extraction efficiency increased from 61 to 95% as the duration increased from 5 to 20 min. As the reaction time was extended to 35 min, the extraction efficiency remained nearly constant (Figure 4c).

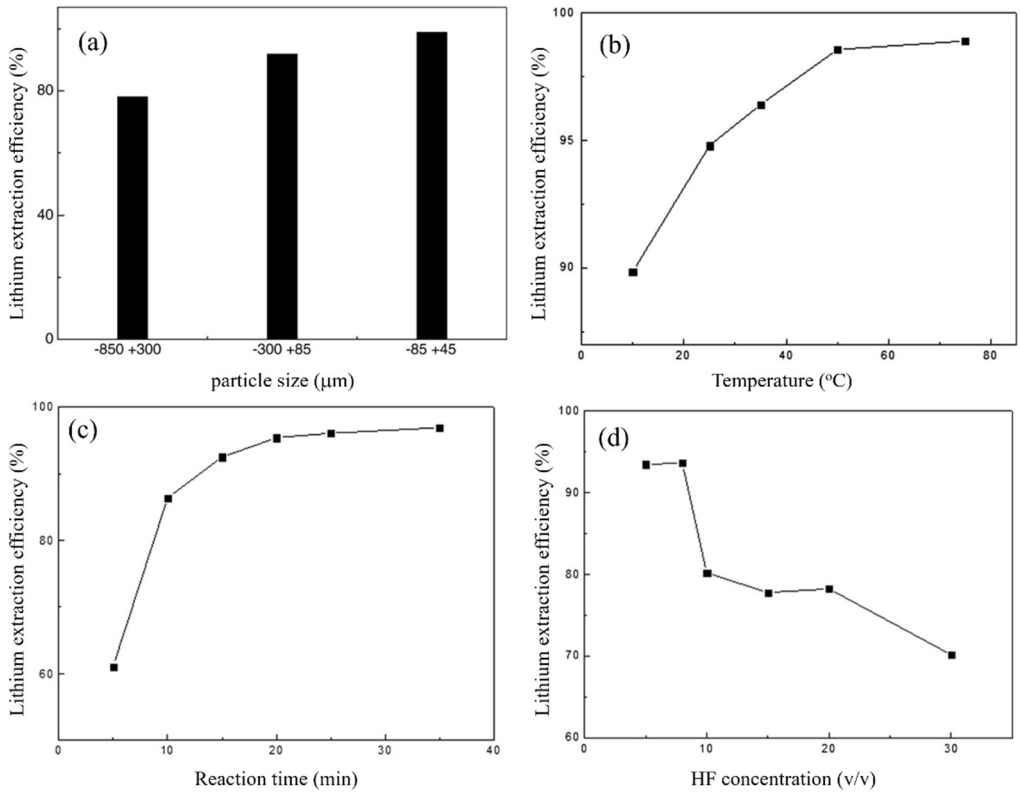

Figure 4. (**a**) Effect of particle size on the Li extraction efficiency. (**b**) Effect of leaching temperature on the Li extraction efficiency. (**c**) Effect of reaction time on the Li extraction efficiency. (**d**) Effect of HF concentration on the Li extraction efficiency. Adapted with permission from [11].

A series of leaching experiments from 5 to 30% (v/v) HF concentrations were performed to explore the influence of the HF concentration on Li extraction, with the following conditions of the leaching process: the solid-to-liquid ratio was 1.82% (w/v), stirring speed was 330 rpm, temperature was 75 °C, and reaction duration was 35 min. With an increase in the HF concentration, a decrease in the extraction efficiency was observed (Figure 4d). The extraction efficiency was slightly affected by the solid-to-liquid ratio. When the solid-to-liquid ratio exceeded 1.82% (w/v), the extraction efficiency of Li remained constant, and this solid-to-liquid ratio was considered optimal.

Figure 5 shows the Li recovery steps from β-spodumene using HF acid leaching. Given the low concentration of HF utilized in the approach (7%), safety concerns about the use of HF were greatly reduced. The key disadvantage of this approach was a very low solid-to-liquid ratio during HF leaching.

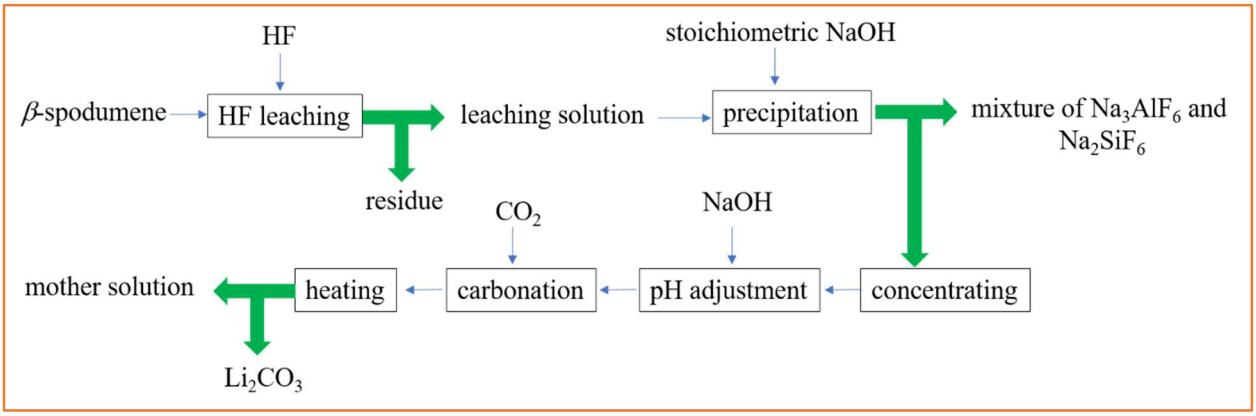

Figure 5. Li recovery steps from β-spodumene using HF acid leaching. Adapted (modified) with permission from [11,21].

2.1.3. Nitric Acid

Hunwick proposed a new method involving the combination of β-spodumene or other Li-containing silicate minerals with HNO_3 under a high temperature (170 °C) and pressure (2 MPa) [48]. This process resulted in the production of lithium nitrate ($LiNO_3$) and the generation of pyrophyllite as a secondary product. The primary reaction that characterizes the leaching process is:

$$LiAlSi_2O_6 + HNO_3 \xrightarrow{170\ ^\circ C \text{ and } 2\ MPa} LiNO_3 + AlSi_2O_5(OH) \quad (10)$$

At these conditions, the method achieved 95% recovery in an hour using a laboratory-scale reactor. At the expense of recovery, the process can also take place at atmospheric pressure and lower temperatures, ranging from 100 to 120 °C. Using HNO_3 precursors (NO_x, oxygen, and water vapor), a comparable process can be carried out at greater temperatures, ranging from 170 to 200 °C:

$$2LiAlSi_2O_6 + 2NO + 1.5O_2 \rightarrow 2LiNO_3 + 2AlSi_2O_5(OH) \quad (11)$$

The reaction is performed to ensure the gas mixture remains in contact with the solid aluminosilicate. When lithium nitrate crystallizes, it can be decomposed at temperatures above 600 °C to obtain oxygen, lithium oxide, and nitric oxide.

2.1.4. Hydrochloric Acid

The use of hydrochloric acid as a leaching agent for β-spodumene (obtained after decrepitation) has been proposed [49]. The concentrate was pulverized to 75 µm and then added to 20% HCl (w/w). In this method, the process is carried out in a chlorination kiln at

108 °C and atmospheric pressure for 8 h. However, to achieve higher recoveries with HCl, a larger concentration of reagent is required, making the process excessively costly in terms of energy and chemical expenses [50].

2.2. Chlorinating Method

Another useful method for producing water-soluble chlorides is chlorination, due to its strong reactivity with metal oxides and silicates. Various chlorination procedures have been used to selectively extract Li as lithium chloride at extreme temperatures from lithium-bearing ores, but the process is complicated and needs highly corrosion-resistant equipment.

2.2.1. Chlorine Gas

Barbosa et al. investigated the extraction of Li using chlorination roasting of β-spodumene at temperatures ranging from 1000 to 1100 °C for times ranging from 0 to 180 min [20]. The experiments were carried out at ≥1000 °C with a 100 mL/min Cl_2 supply, and the total extraction of Li as LiCl was achieved after 150 min at 1100 °C. Equation (12) describes the interaction between β-spodumene and Cl_2:

$$12\beta - LiAlSi_2O_6(s) + 6Cl_2(g) \rightarrow 3O_2(g) + 12LiCl(l) + 2Al_6Si_2O_{13}(\text{mullite}) + 20SiO_2(\text{cristobalite}), \quad \Delta G^o_{1100\,^\circ C} = -707.88\ \text{kJ/mol} \tag{12}$$

The observed reaction exhibited non-catalytic behavior and involved the interaction between a gas and a solid. The reaction can be described by the sequential nucleation and growth model. Also, it was discovered that LiCl products and other chlorides generated by impurities (e.g., $FeCl_3$ and $CaCl_2$) volatilize together during extraction, contaminating the product that must be further processed. The employed α-spodumene sample (San Luis, Argentina) had a mineralogical composition of 95.5% α-spodumene and 4.5% quartz. The ore was pulverized in a ring mill, sieved to less than a 50 µm particle size, and then calcined at 1180 °C for two hours to produce β-spodumene (tetragonal).

The reactor bed constituted a quartz tube with an outside diameter of 16 mm, a wall thickness of 1 mm, and a length of 440 mm that was placed within an electric furnace with a temperature controller. The sample was enclosed inside the reactor in a quartz crucible (length 70 mm, width 10 mm, and depth 6 mm), as illustrated in Figure 6a. A Chromel–Alumel thermocouple was used to measure the temperature to within ±5 K. Through Teflon tubing, Cl_2 from a cylinder was delivered to the quartz tube's inlet. The flow rate was controlled using mass flowmeters and metering valves.

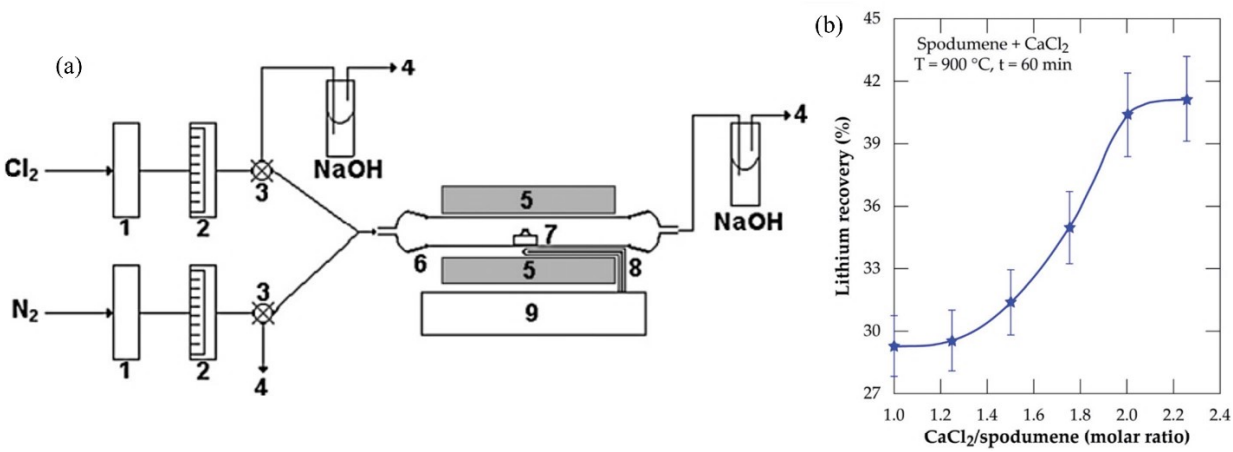

Figure 6. (**a**) Fixed-bed reactor. (1) H_2SO_4 dryers, (2) flowmeters, (3) three-way valves, (4) venting, (5) electric furnace, (6) quartz tubular reactor, (7) quartz crucible, (8) thermocouple, and (9) temperature controller. Adapted with permission from [20]. (**b**) Lithium recovery % vs. $CaCl_2$/spodumene molar ratio for samples treated at 900 °C for 60 min. Adapted with permission from [51].

The direct application of Cl_2 at elevated temperatures presents considerable safety risks and requires the use of expensive materials, complicating the process. High-temperature (1000 °C) roasting consumes significantly more energy than acidic methods, especially when phase transfer roasting (1180 °C, 2 h) is also required. Furthermore, because the roasting can occur at a higher temperature (1100 °C), which also facilitates decrepitation, this procedure, given the aggressive character of Cl2, can be used for the direct processing of α-spodumene [21].

2.2.2. Chloride Routes

Calcium chloride has been employed as a chlorinating agent in metal extraction from various sources [52,53]. Furthermore, in the presence of silica, calcium chloride has been proven to be the most effective chlorinating agent. As a result, calcium chloride was tested as a chlorinating agent for the extraction of Li as lithium chloride from β-spodumene [54]. $CaCl_2$ can react with β-spodumene at a lower temperature, starting at 700 °C, and is non-toxic and less corrosive than Cl_2. The extent of Li conversion reached 90.2% under optimum conditions of 900 °C, 2 h, with an ore/$CaCl_2$ molar ratio of 0.5. During the chlorinating roasting, β-spodumene was also decomposed and converted to LiCl, SiO_2, and $CaAl_2Si_2O_8$. The spodumene ore (San Luis, Argentina) contained 7.2% Li_2O and less than 2% impurities, such as Fe_2O_3, CaO, and MgO. This rock ore was pulverized in a ring mill, sieved to a particle size of less than 50 µm, then calcined at 1180 °C for 2 h to convert it to its β-phase. The mixture was then combined with calcium chloride in a mortar to achieve a β-$LiAlSi_2O_6$/$CaCl_2$ molar ratio of 1:2. The mixture was dried in a muffle furnace at 200 °C until it reached constant mass. Because calcium chloride is hygroscopic, efforts were made to keep it dry. The roasting was carried out in a nitrogen-fed fixed-bed reactor. At 60 °C, the roasted sample was leached with water.

Another work reported on α-spodumene direct chlorination using calcium chloride followed by water leaching of the residue to recover Li [51]. The α-form was the sole polymorph found in leftovers after leaching, implying that the extraction is performed straight from the α-phase. However, the generation of a metastable β-form followed by a rapid synthesis of lithium chloride is also suspected. Under ideal conditions of a calcium chloride/spodumene molar ratio of 2.0 and a 60 min 1000 °C treatment, nearly 90% lithium chloride was extracted, with 85% returned to the leaching solution and the remaining escaping with the off-gas. The effect of the $CaCl_2$/spodumene molar ratio (Figure 6b), temperature, and chlorinating time on Li recovery was also explored.

Sodium chloride, a cost-effective and readily available compound, has been employed as a chlorinating agent for the purpose of extracting Li from β-spodumene. This extraction process is conducted under both high-pressure conditions and inside an alkaline environment (Figure 7, Equation (13)) [55].

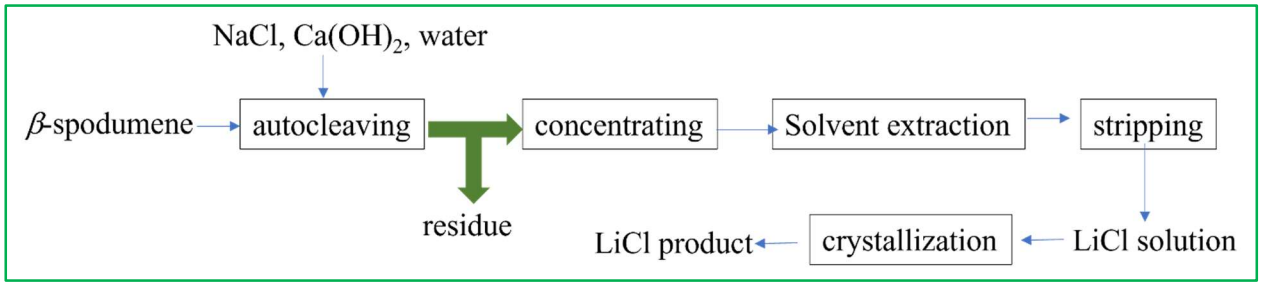

Figure 7. Li recovery process from β-spodumene by the chlorinating method, with NaCl as the chlorinating agent. Adapted (modified) with permission from [21,55].

This research examined multiple parameters: concentrations of NaCl and $Ca(OH)_2$, temperature, pulp density, time, and ore size, to evaluate the extraction of Li. The results indicated that a nearly complete extraction of Li was achieved within around 3.5 h of

leaching, with the ore size being 100% < 42 μm. The process of directly crystallizing the leaching solution, which was obtained through autoclaving, was also carried out in order to produce LiCl with a purity level of 91%:

$$\beta - Li_2O{\cdot}Al_2O_3{\cdot}4SiO_2 + 2NaCl + 2H_2O \rightarrow 2LiCl + Na_2O{\cdot}Al_2O_3{\cdot}4SiO_2{\cdot}2H_2O \quad (13)$$

There has also been a report of utilizing NH_4Cl to directly roast α-spodumene for Li extraction [56]. When α-spodumene was sintered with $CaCO_3$ and NH_4Cl at a 1/3/1 ratio at 750 °C, almost 97% Li could be converted to LiCl (Equation (14)):

$$\alpha - Li_2O{\cdot}Al_2O_3{\cdot}4SiO_2 + 4CaCO_3 + 2NH_4Cl \rightarrow 2LiCl + 4CaSiO_3 + Al_2O_3 + 4CO_2 + 2NH_3 + H_2O \quad (14)$$

2.3. Carbonate Roasting and Autoclaving Method

The Li extraction using the carbonate method relies on the process of ion exchange between Li^+ and the metal ion present in carbonate, predominantly Na^+. Equation (15) represents the reaction process between β-spodumene and sodium carbonate (Na_2CO_3) [57]:

$$\beta - Li_2O{\cdot}Al_2O_3{\cdot}4SiO_2 + Na_2CO_3 + nH_2O \rightarrow Li_2CO_3 + Na_2O{\cdot}Al_2O_3{\cdot}4SiO_2{\cdot}nH_2O \quad (15)$$

The aforementioned reaction has been successfully accomplished using the process of roasting within a temperature range of 450–750 °C (a solid–solid reaction mechanism). Alternatively, autoclaving at approximately 225 °C has also been employed to obtain the desired outcome [57]. Consequently, the reaction will yield Li_2CO_3 and analcime. Due to its limited solubility, particularly under elevated temperatures, Li_2CO_3 has the potential to precipitate and remain as residue subsequent to roasting or autoclaving processes. In order to achieve solubility and separability with residue, such as in the case of analcime, a common approach involves the utilization of a carbonation process. This process aims to convert Li_2CO_3 into lithium bicarbonate ($LiHCO_3$; as shown in Equation (16)), which may then be removed from the mixture using filtration. Subsequently, the $LiHCO_3$-rich filtrate can be subjected to heating (as described in Equation (17)) in order to obtain high-purity Li_2CO_3:

$$Li_2CO_3(s) + H_2O + CO_2(g) \rightarrow 2LiHCO_3(aq), \Delta G^o_{25\,^\circ C} = -4.50\ kJ/mol \quad (16)$$

$$2LiHCO_3(aq) \rightarrow \overrightarrow{heating} \rightarrow Li_2CO_3(s) + H_2O + CO_2(g), \Delta G^o_{95\,^\circ C} = -6.10\ kJ/mol \quad (17)$$

Figure 8a illustrates the steps for extracting Li from β-spodumene via autoclaving with Na_2CO_3 [57]. In this method, ~94% Li was extracted from β-spodumene.

The α-spodumene (Jiangsu, China) was transformed to β-spodumene first by roasting it for 30 min in an electrical muffle furnace at 1050 °C for crystal transformation. A 1 L stainless-steel autoclave was used for the sodium carbonate autoclave process. A representative model of a general-purpose autoclave that is employed in hydrothermal or digestion processes is shown in Figure 8e. To improve agitation in this experiment, 20 steel balls (10 mm) were placed in the autoclave. Na_2CO_3 solution and β-spodumene were added to the autoclave. By autoclaving with Na_2CO_3 at a L/S ratio of 4 mL/g, Na/Li ratio of 1.25, and 225 °C for 60 min, 94% Li was extracted from β-spodumene, and roughly 70% Li_2CO_3 was recovered from $LiHCO_3$ solution by heating at 90 °C for 1 h, with a purity of 99.6%. The effect of the L/S ratio, sodium-to-lithium ratio, agitation, and reaction temperature on the lithium carbonate conversion efficiency was studied and shown in Figure 8b–e. The main disadvantages of this method are the high cost of autoclaving and heating, the several stages involved, and the low conversion efficiencies in leaching and generating lithium carbonate.

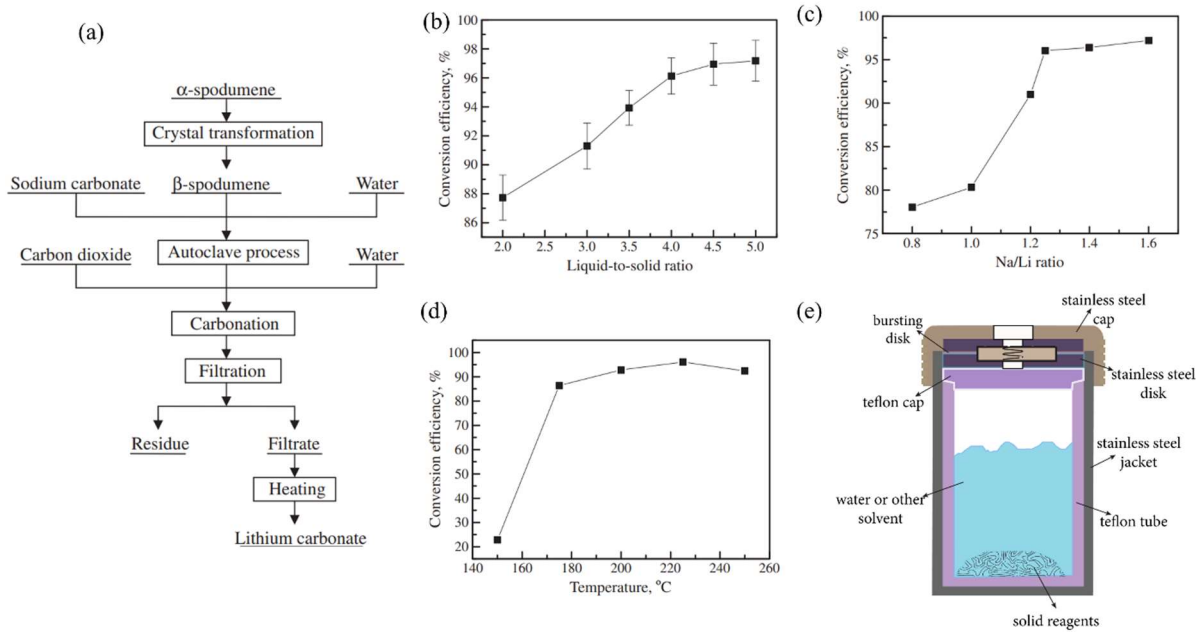

Figure 8. (**a**) A schematic representation of the autoclaving procedure employed for the extraction of lithium carbonate from spodumene. (**b**) Lithium carbonate conversion efficiency and L/S ratio. Conditions: Na/Li ratio 1.5, stirring speed 350 rpm, reaction temperature 230 °C, and reaction time 90 min. (**c**) The Na/Li ratio affects the lithium carbonate conversion efficiency. Conditions: L/S ratio 4, stirring speed 350 rpm, reaction temperature 230 °C, and reaction time 90 min. (**d**) Lithium carbonate conversion efficiency vs. reaction temperature. Conditions: L/S ratio 4, Na/Li 1.25, stirring speed 300 rpm, and reaction time 90 min. Adapted with permission from [57]. (**e**) General-purpose autoclave that is employed in hydrothermal or digestion processes.

Another method for autoclaving β-spodumene using Na_2CO_3 has been reported [58]. In this approach, a further leaching step was utilized to convert Li_2CO_3 into soluble LiOH (Equation (18)), which was then crystallized as $LiOH{\cdot}H_2O$ after impurity removal using ion exchange (Figure 9). It has been reported that the purity of the product obtained in one crystallization stage was as high as >56.5% LiOH, and that the Li extraction reached up to 94%. This procedure presents an alternative approach for subsequent treatment after the carbonate autoclaving of β-spodumene, whereby the production of the LiOH product is achieved directly, instead of Li_2CO_3. The process of leaching in an alkaline environment has the potential to effectively eliminate contaminants, such as Al, Ca, Mg, Fe, and P. This method offers a distinct advantage when compared to the less specific acid-leaching process. Nevertheless, the residue resulting from this procedure is a mixture containing Na, Al, Si, and Ca. Consequently, additional treatment is necessary to recover these elements, with a special focus on Al:

$$Li_2CO_3(s) + Ca(OH)_2(s) \rightarrow 2LiOH(aq) + CaCO_3(s) \quad (18)$$

Similarly, a nitric acid pressure-leaching technique was adapted to extract Li from β-spodumene [59]. In the experiment, the raw material was mixed with a HNO_3 solution (concentration of 0.2–3 mol/L) and made to react at a predetermined temperature (120–220 °C) and time (30–180 min) in an autoclave. At 200 °C, with an initial HNO_3 concentration of 1 mol/L, L/S ratio of 2.5 mL/g, and a holding time of 30 min, 95% Li was extracted with low amounts of impurities. Figure 9b–d show the effect of the nitric acid concentration, L/S ratio, and holding time, respectively, on Li extraction. Pressure leaching preserved β-spodumene's aluminum-silicate cage structure, allowing H^+ to readily exchange with Li^+ and create $HAlSi_2O_6$. The leached liquid was then thermally decomposed at 250 °C to separate Li and aluminum.

A direct solid-state reaction involving α-spodumene (North Carolina), Na_2CO_3, and Al_2O_3 at a low temperature of 750 °C and a short hold period of 4 h can produce Li_2CO_3 with a yield of over 90% [60]. The inclusion of Al_2O_3 is crucial for reducing the amount of Li_2SiO_3 produced when only Na_2CO_3 is employed. To prepare the samples, the spodumene concentrates (particle size < 75 µm) were mixed with Na_2CO_3 and Al_2O_3 nano-powder using a planetary ball mill at 250 rpm/12 h and dried in a 70 °C oven overnight before pelletization. The pellets were sintered in air at 750 °C for various durations (10 min, 30 min, 2, 4, and 8 h) before cooling naturally to room temperature. After 30 min at 750 °C, Li extraction was nearly complete, yielding 85% Li_2CO_3 (Figure 9e).

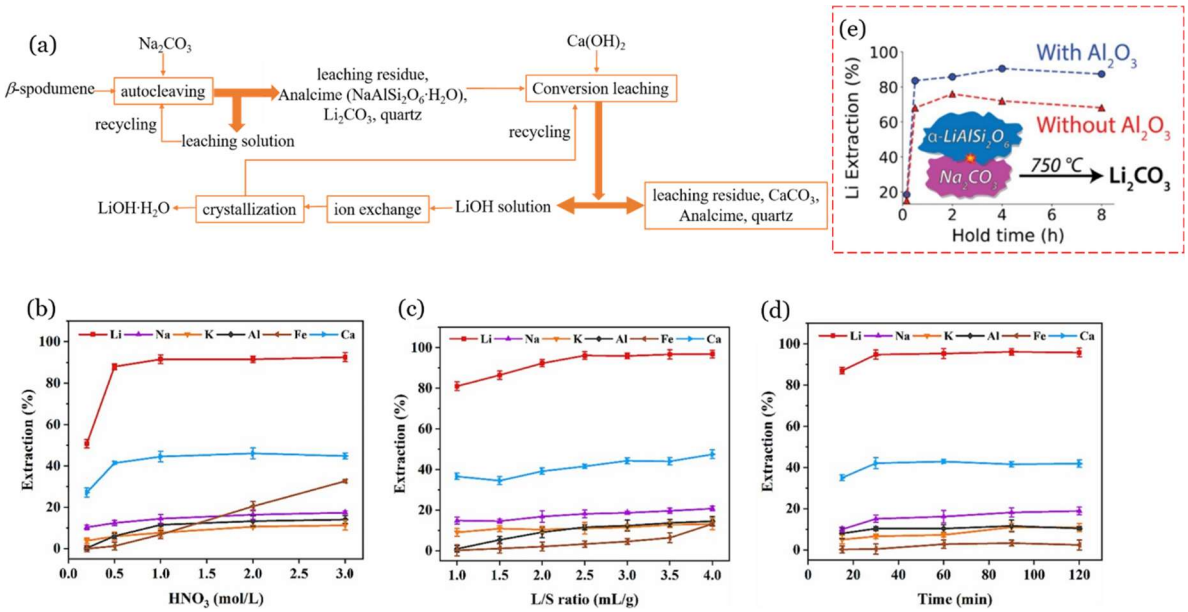

Figure 9. (**a**) Li recovery from β-spodumene via carbonate autoclaving. Adapted with permission from [21]. (**b**–**d**) Nitric acid pressure leaching. (**b**) Effect of nitric acid concentration on element extraction at 140 °C with a L/S ratio of 3 mL/g and a reaction time of 90 min. (**c**) Effect of the L/S ratio on element extraction at 200 °C, nitric acid concentration of 1 mol/L, and holding time of 90 min. (**d**) Effect of holding time on element extraction at 200 °C, L/S ratio of 2.5 mL/g, and initial nitric acid concentration of 1 mol/L at 15 to 120 min of holding time [59]. (**e**) The % of Li extracted from α-spodumene in the form of Li_2CO_3 vs. the time at 750 °C for two distinct reactions [60].

2.4. Alkali Methods

The ability of alkali to chemically react with and disrupt the Si-O bond, resulting in the dissolution of SiO_2 in a solution, is widely recognized. This dissolution process is observed to intensify as the alkalinity and temperature of the solution increase. Following this, several teams employed alkali as a means of directly extracting Li from α-spodumene.

Alkaline Hydrothermal Treatment

Xing et al. devised a method for extracting Li from α-spodumene while also synthesizing hydroxysodalite zeolite [61]. The α-spodumene was transformed into hydroxysodalite ($Na_8[AlSiO_4]_6(OH)_2 \cdot nH_2O$) via hydrothermal alkaline treatment, and the Li in α-spodumene was released into the solution and recovered via precipitation with Na_2CO_3. Under optimal conditions, a Li extraction efficiency of 95.8% was obtained: temperature 250 °C, NaOH concentration 600 g/L, liquid/solid ratio 5:1, stirring speed 500 rpm, and reaction time 2 h. The predicted reaction is shown in Equation (19). A vertical autoclave was used to execute the hydrothermal alkaline treatment of α-spodumene. In the autoclave, the α-spodumene ore was first combined with a NaOH solution at a certain L/S ratio. The slurry was stirred. The temperature was kept under control by adjusting the heating and cooling water. The slurry was filtered after the hydrothermal alkaline treatment to separate

the Li solution and solid product. The solid product was cleaned with deionized water and dried in an oven. Desilication was also performed in the autoclave, with the stirring rate set at 500 rpm. Following this, the remaining Li in the solution was concentrated and subsequently precipitated as lithium carbonate (Li_2CO_3). Figure 10e presents a flowchart illustrating the process of Li extraction and subsequent recovery.

$$6\alpha - LiAlSi_2O_6 + 14NaOH \rightarrow 2Na_4Al_3Si_3O_{12}(OH) + 3Li_2SiO_3 + 3Na_2SiO_3 + 6H_2O \quad (19)$$

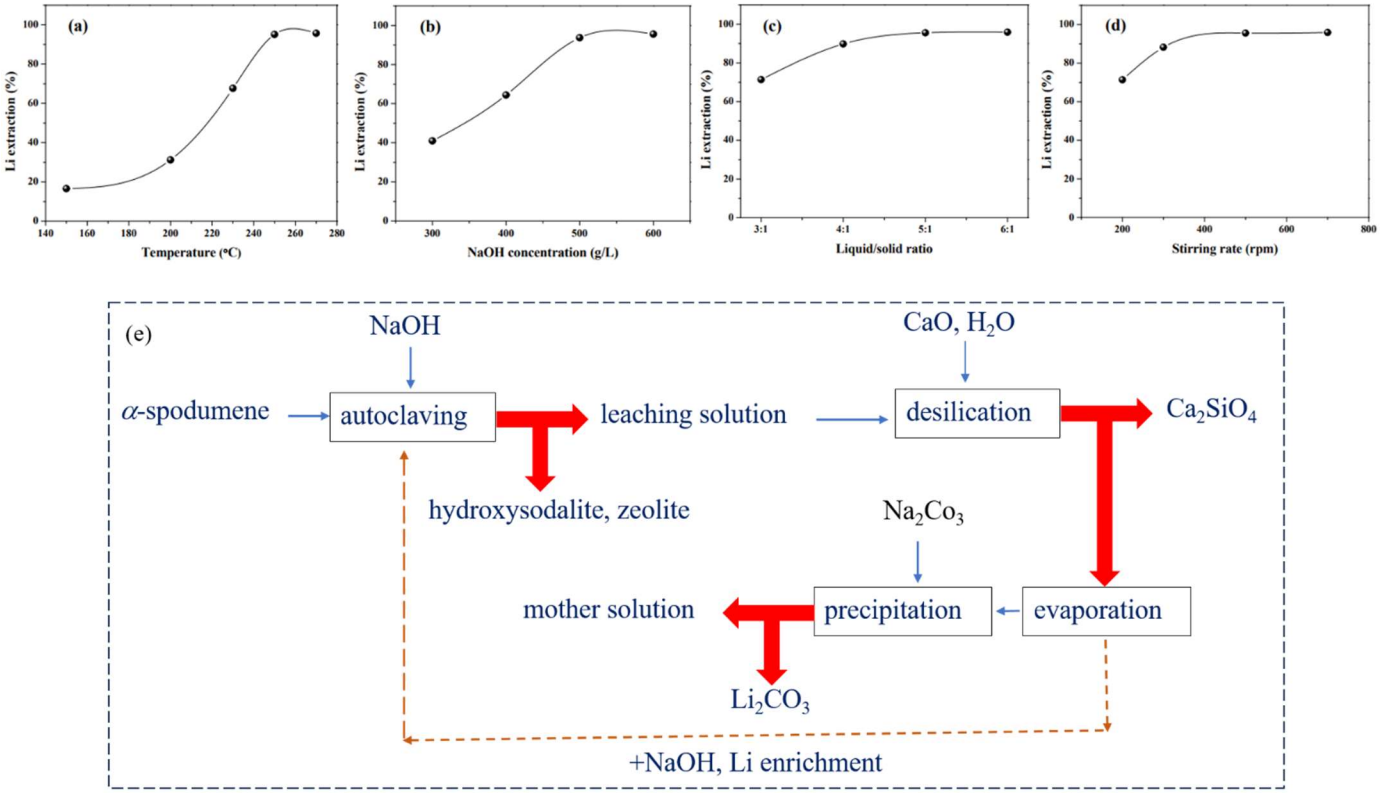

Figure 10. Li extraction and hydroxysodalite zeolite synthesis. Effects of (**a**) temperature, (**b**) NaOH concentration, (**c**) liquid/solid ratio, and (**d**) stirring rate [61]. (**e**) Steps for Li recovery from α-spodumene by using NaOH. Adapted (modified) with permission from [21].

Further, the effects of a temperature, NaOH concentration, L/S ratio, stirring rate, and leaching time on the extraction of Li were analyzed and shown in Figure 10a–d. By directly processing α-spodumene with NaOH, phase transfer at high temperatures was avoided, and a high Li extraction efficiency was attained. However, given the nature of the alkali–silica reaction, this approach frequently results in significant caustic consumption.

Qui et al. employed a hydrothermal alkaline treatment to investigate a direct decomposition of α-spodumene using a NaOH solution [62]. The results revealed that, under specific conditions, the Li present in the α-spodumene converted into an intermediate product, Li_2SiO_3, which existed in the form of a solid phase. The overall extraction efficiency of Li_2O was found to be 87.3%. This value includes the extraction efficiency of Li_2O that was leached into the liquid phase (7.6%) and converted into Li_2SiO_3 (79.7%) obtained under the optimal experimental conditions: a stirring speed of 500 rpm, a leaching temperature of 250 °C, a mass ratio of NaOH/ore of 1.5, an initial NaOH concentration of 25 wt%, and a leaching time of 24 h. The extraction of the Li from Li_2SiO_3 can be achieved using acid leaching, followed by precipitation using Na_2CO_3. The residual liquid obtained following the hydrothermal alkaline treatment was utilized again for the subsequent hydrothermal alkaline cyclic leaching, using the same conditions as mentioned above. Throughout three iterations of alkaline treatment, the decomposition of α-spodumene exhibited consistent

stability, resulting in an approximate total extraction efficiency of 86% for Li_2O (with about 84% being transformed into Li_2SiO_3).

In the study, the spodumene concentration (Australia) was crushed in a jaw crusher, processed in a ball mill, and screened to 200 mesh (less than 0.074 mm). Known amounts of spodumene concentrate and NaOH solution were mixed and charged into the autoclave (250 mL vertical Zr-lined autoclave) for each hydrothermal experiment. The mixture was then heated to the desired temperature while being constantly stirred for a set period of time. Following hydrothermal treatment, the autoclave slurry was removed and centrifuged to separate the pregnant solution from the residue. The residue was washed twice with deionized water before being centrifuged and filtrated before drying at 110 °C. The leaching pregnant solution and washing solution were combined during the analysis of the Li_2O content that had been leached into the solution. Then, 0.100 g of alkaline residue was weighed and leached with 50 mL of 2 mol/L HCl solution at 60 °C for 4 h to determine the amount of Li_2O converted to Li_2SiO_3 in the residue.

Further effects of the stirring speed, leaching temperature, mass ratio of NaOH/ore, and initial NaOH concentration on the extraction efficiency of Li_2O were analyzed (Figure 11a,b—only the leaching temperature and mass ratio are shown). The use of alkaline processing to recover the Li contained in pegmatite minerals, such as spodumene, may have advantages over the current acid process, particularly by allowing the replacement of expensive inputs, such as sulfuric acid (H_2SO_4) and soda ash (Na_2CO_3) with limestone ($CaCO_3$) or hydrated lime ($Ca(OH)_2$), both of which are widely available and inexpensive.

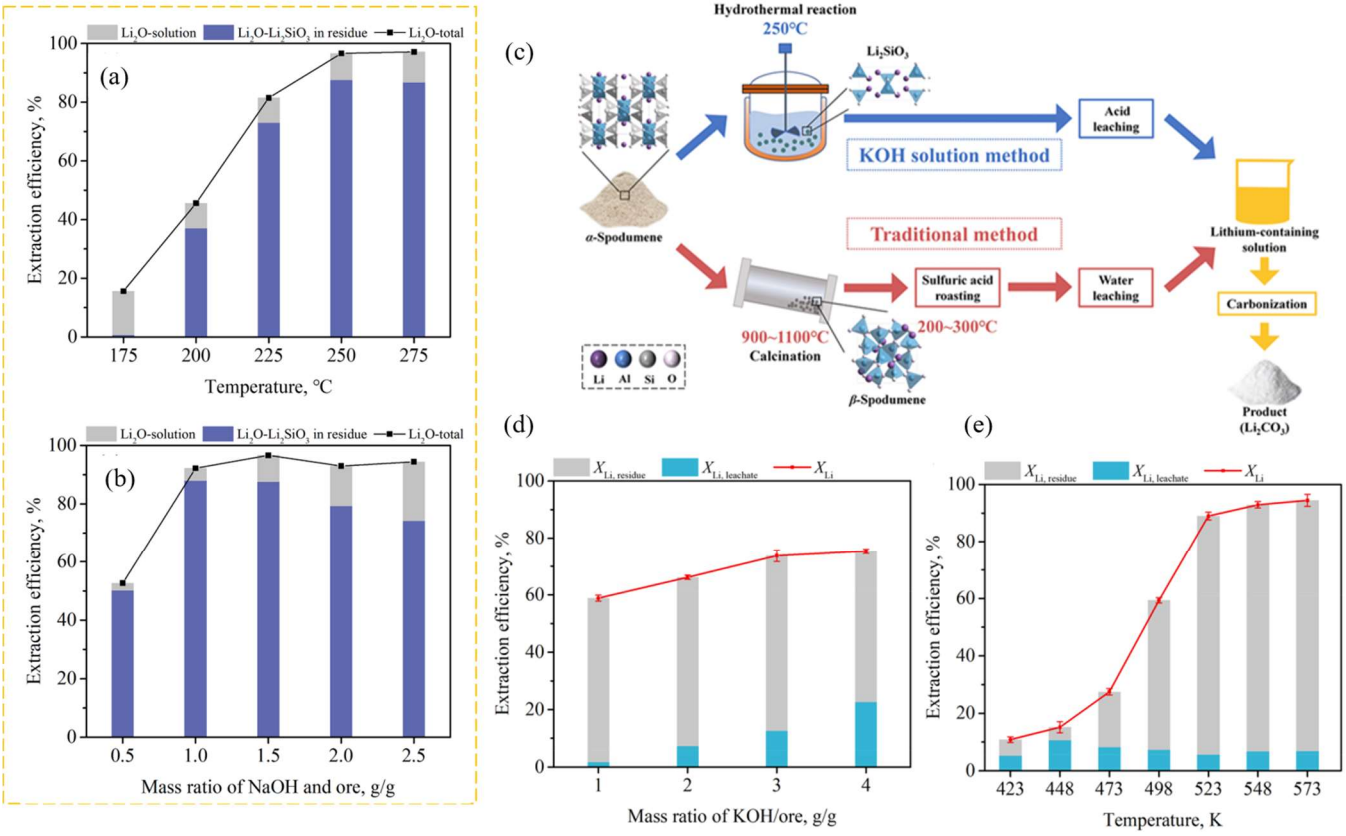

Figure 11. (**a**,**b**) Li extraction in NaOH solution. (**a**) Effect of leaching temperature. (**b**) Mass ratio of NaOH/ore (conditions: 500 rpm, NaOH/ore = 1.5 g/g, initial NaOH concentration = 25 wt%, t = 24 h) [62]. (**c**–**e**) Li extraction in KOH solution. (**c**) Extraction steps. The effects of the (**d**) mass ratio of KOH/ore and (**e**) leaching temperature on the extraction efficiency. Adapted with permission from [63].

The same author demonstrated that a KOH solution may directly break down the structure of α-spodumene, resulting in the simultaneous generation of new solid-phase products of Li_2SiO_3 and $KAlSiO_4$ [63]. Under optimal conditions, the total Li extraction efficiency could reach 89.9%, with 84.1% converted into Li_2SiO_3 and 5.8% converted into the liquid phase: an initial KOH concentration of 50 wt%, a stirring speed of 500 rpm, a mass ratio of KOH/ore of 2:1, a leaching temperature of 523.15 K, and a leaching time of 16 h. The spodumene concentrate (from China) was crushed, ground, and sieved to ∼60 mesh (below 0.25 mm). The experimental steps are quite similar to the study discussed above. The effects of stirring speed, KOH/ore mass ratio, leaching temperature, and leaching time on the extraction efficiency were studied (Figure 11—only the effect of leaching temperature and the mass ratio of NaOH/ore are shown). When compared to the NaOH technique to produce Li_2SiO_3 [62], this outcome demonstrated advantages in terms of reaction time and leaching pressure. This approach eliminates the need for high-temperature calcination, concentrated sulfuric acid roasting, and the difficulty of isolating Li from leachate with a high potassium level.

Song et al. demonstrated an autoclave digestion method for directly extracting Li from α-spodumene using an alkaline solution with the addition of CaO [64]. The ideal operating parameters for the Li extraction efficiency of 93.3% were a CaO/ore mass ratio 0.5:1, leaching time of 6 h, NaOH concentration of 400 g/L, temperature of 250 °C, and L/S ratio of 7 mL/g. Li_3PO_4 was formed by precipitating the Li in the leaching solution with Na_3PO_4. The leaching of α-spodumene (Sichuan, China) was subjected to digestion by placing the α-spodumene/NaOH solution mixture in a 600 mL Monel alloy autoclave. The CaO was added to enhance the leaching efficiency. The effects of the CaO/ore mass ratio, leaching temperature, NaOH concentration, L/S ratio (NaOH/ore), and leaching time on the extraction efficiency of Li were studied. The leaching temperature, the mass ratio of the added CaO to ore, and the concentration of NaOH all significantly impacted the efficiency of Li extraction (Figure 12b–e).

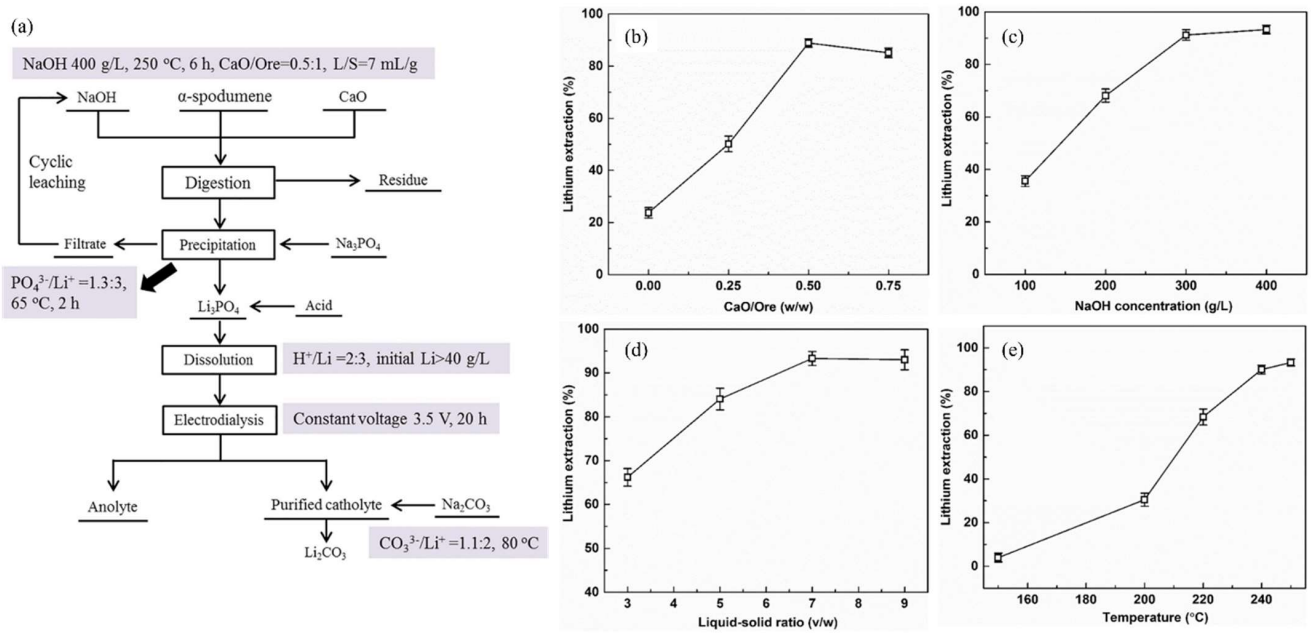

Figure 12. (**a**) Process flowchart for extracting Li from α-spodumene. (**b**) Effect of the mass ratio of CaO to ore on Li extraction. T = 250 °C, NaOH = 400 g/L, t = 4.5 h, L/S ratio (NaOH/Ore) = 7 mL/g. (**c**) Effect of NaOH concentration on Li extraction. T = 250 °C, mass ratio of CaO/ore = 0.5:1, t = 6 h, L/S ratio (NaOH/Ore) = 7 mL/g. (**d**) Effect of L/S ratio (NaOH/Ore) on Li extraction. T = 250 °C, mass ratio of CaO/ore = 0.5:1, t = 6 h, NaOH = 400 g/L. (**e**) Effect of leaching temperature on Li extraction. Mass ratio of CaO/ore = 0.5:1, t = 6 h, NaOH = 400 g/L, L/S ratio (NaOH/Ore) = 7 mL/g. Adapted with permission from [64].

Salt roasting is an alternative to high-temperature calcination, as it lowers the roasting temperature of α-spodumene and provides excellent Li-leaching recovery by turning it into water/acid-soluble Li compounds. In that direction, nine reagents consisting of alkali metals (Group IA), alkaline earth metals (Group IIA), and ammonium ($NH4^+$) salts were tested for roasting and phase transformation of α-spodumene into phases that are soluble in acid or water to directly extract Li from α-spodumene [65]. In order to achieve this, a series of sequential processes, including roasting, water leaching, and acid leaching, were conducted. The leaching recovery data revealed that the three reagent categories' roasting efficacy was ordered as follows: Group IA > Group IIA > NH_4^+. The NaOH roasting–water-leaching–acid-leaching process achieved 71% and 88% water-leaching and total leaching recovery values, respectively, under non-optimized parameters of a roasting temperature of 320 °C, a NaOH/spodumene ratio of 1.5:1, and a roasting period of 2 h (Figure 13a). The roasting of Na_2CO_3 at a temperature of 851 °C resulted in a significant overall leaching recovery of Li, reaching 76%. However, the recovery of Li through water leaching was very low, at 27%. This can be attributed to the limited solubility of Li_2CO_3, as well as the formation of $NaAlSiO_4$ and the subsequent extensive sintering of the roasted sample. The main minerals found in the spodumene sample (Tin-Spodumene Belt, North Carolina) were spodumene (20% with 1.6% Li_2O), quartz (30%), feldspar (43%), and mica (5%). The concentration was composed of 6% Li_2O and <1% Fe_2O_3. In each roasting trial, a 2 g sample of spodumene concentrate was combined with 3 g of the designated reagent, resulting in a reagent-to-spodumene ratio of 1.5:1. The mixture was placed in a Zr crucible and subjected to heating at the reagent's melting point (i.e., NaOH: 318 °C, Na_2Co_3: 851 °C, NaCl: 801 °C, KOH: 360 °C, etc.).

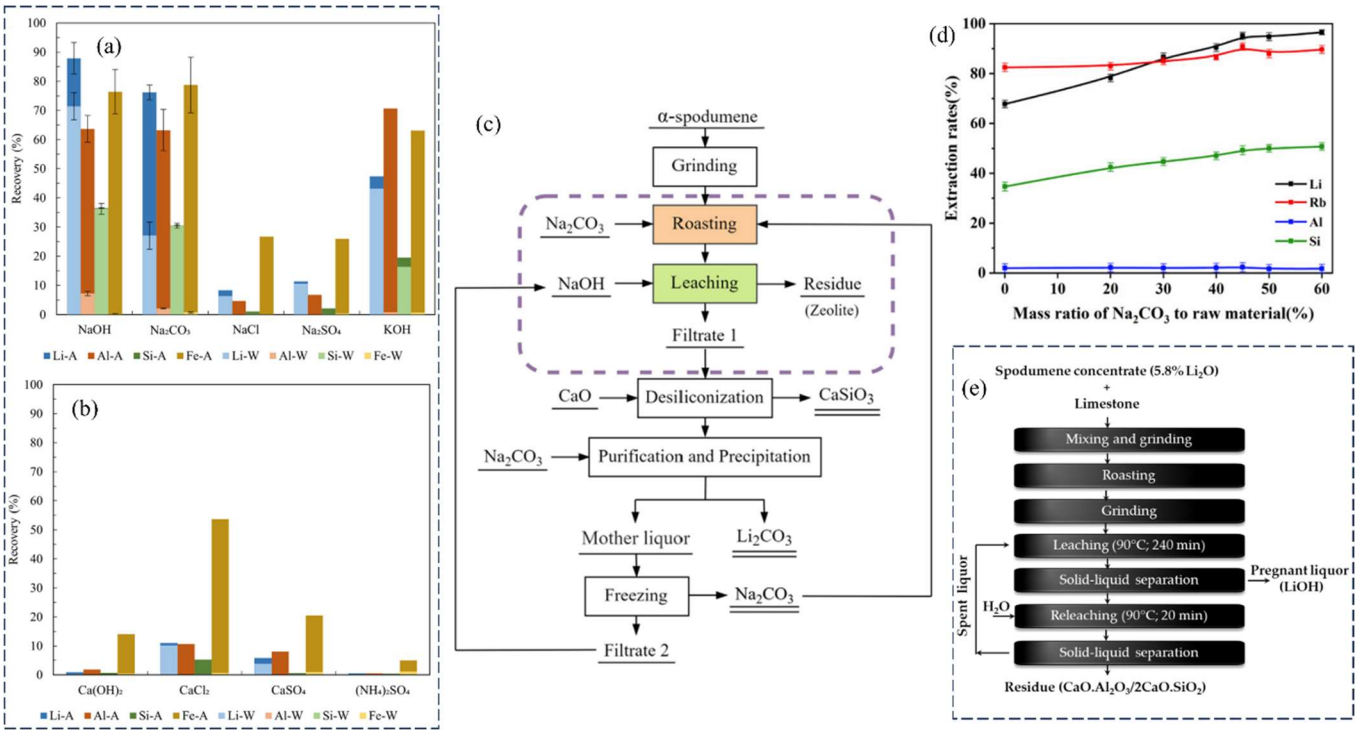

Figure 13. (**a**,**b**) Salt roasting−leaching. Water (W) and acid (A) leaching recovery of Li and other elements from α-spodumene roasted with typical reagents of (**a**) Group IA and (**b**) Group IIA and NH_4^+. Adapted with permission from [65]. (**c**,**d**) Carbonate roasting, water quenching, and leaching. (**c**) Process flowsheet for extracting Li and Rb from α-spodumene. (**d**) Effect of the mass ratio of Na_2CO_3 to ore on the extraction of Li, Rb, etc. [66]. (**e**) Calcination decrepitation reaction of spodumene with limestone. Block schematic illustrates the typical processing steps [67].

The NaOH roasting method provides low-temperature roasting and excellent Li recovery, particularly in water leaching. As a result, this technique avoids both high-temperature calcination and acid-baking stages, as well as the CO_2 emissions, significant energy and acid use, and environmental concerns associated with them.

Similar to the carbonatizing roast of Li-bearing ores by Maurice and Olivier [68], the carbonate roasting approach has recently been developed and tested for the extraction of Li and Rb. Zhou et al. proposed a direct Li extraction process for α-spodumene (particle size D_{10} ~2.595 µm, D_{50} ~31.818 µm, and D_{90} ~135.467 µm) via (1) sodium roasting, (2) water quenching, and (3) strengthening leaching (Figure 13c) [66]. The findings indicated that at high temperatures (1000–1300 °C), α-spodumene interacted directly with Na_2CO_3 to produce Li_2SiO_3, $NaAlSiO_4$, and Na_2SiO_3. The combined action of sodium roasting and water quenching broke the stable aluminosilicate structure in α-spodumene, which played a substantial role in the release of Li. It was concluded that Na_2CO_3 could increase α-spodumene dissolution. The ideal roasting parameters were established based on the optimization results to be roasting at 1100 °C for 30 min with the addition of 45% Na_2CO_3 (Figure 13d). Li and Rb extraction were 95.9% and 90.3%, respectively, whereas the Al extraction rate was only 1.5%. The extraction rates of Li and Rb increased from 85% to 95% and 80% to 90%, respectively, when the roasting temperature scaled from 1000 to 1100 °C. Rapid cooling of roasted slag induced complete mineral dissociation.

Bragga et al. conducted a lab-scale calcination decrepitation reaction of spodumene (with 5.8% Li_2O; Minas Gerais, Brazil) with limestone [67]. The sample (with a particle size distribution of 6 mm) was pulverized in jaw and roller crushers before being processed in rod and ball mills to a maximum grain size of 100 µm. A series of mass ratios (1:1, 1:2, 1:3, 1:3.5, 1:4, and 1:5) between spodumene and calcitic limestone (particle size of 100 µm) were subjected to heating in a muffle furnace. The mixes were placed into crucibles made of alumina and underwent thermal treatment at a temperature of 1050 °C for 30 min. The calcination decrepitation reaction of spodumene with limestone (roasting process) involves three distinct steps [67]: (i) decomposition of limestone at temperatures ranging from 750 to 800 °C, resulting in the formation of CaO and the release of CO_2, (ii) decrepitation to conversion of α-spodumene into β-spodumene, and (iii) a solid–solid reaction between β-spodumene and CaO particles, with the formation of lithium aluminate and calcium silicate. Steps (ii) and (iii) occur almost simultaneously (at 1050 °C). The resulting product, after cooling, was ground in an agate mortar to a particle size < 100 µm and leached with water at 90 °C, at a solid-to-liquid (S/L) ratio of 10% p/p. The block diagram in Figure 13c illustrates the trials performed. The reactions of the process are presented as follows:

$$\begin{gathered} CaCO_3 \rightarrow CaO + CO_2 \\ Li_2O{\cdot}Al_2O_3{\cdot}4SiO_2 + 8CaO \rightarrow Li_2O{\cdot}Al_2O_3 + 4(2CaO{\cdot}SiO_2) \\ CaO + H_2O \rightarrow Ca(OH)_2 \\ Li_2O{\cdot}Al_2O_3 + Ca(OH)_2 \rightarrow 2LiOH + CaO{\cdot}Al_2O_3 \end{gathered} \tag{20}$$

The best spodumene:limestone mass ratio was 1:5, resulting in a Li recovery of approximately 64%. The Li extraction for a roasting period of 120 min was lower than that for a roasting time of 30 min, most likely due to sintering or vitrification of the resultant product during the roasting, which hampered the extraction of the Li.

McIntosh [69] suggested combining β-spodumene with lime at temperatures of 100 to 205 °C and pressures of 0.35 to 1.73 MPa to produce lithium hydroxide. The filtrate was then concentrated by evaporation and carbonated at around 60 °C:

$$Li_2O{\cdot}Al_2O_3{\cdot}4SiO_2 + CaO + H_2O \rightarrow 2LiOH + CaO{\cdot}Al_2O_3{\cdot}4SiO_2 \tag{21}$$

$$2LiOH + CO_2 \rightarrow Li_2CO_3 + H_2O \tag{22}$$

This method can yield an extraction efficiency of up to 90%. The limestone and lime-based methods remain tempting to the industry. The primary disadvantages are the high cost of energy necessary for spodumene decrepitation, β-spodumene roasting,

and the requirement to grind the roasted product before water leaching for the bulkiest extraction [22].

It has been shown that Li may be extracted directly from α-spodumene using CaO-activated roasting and H_2SO_4 leaching (Figure 14a). The α-spodumene was transformed to β-spodumene, which then interacted with CaO to produce acid-soluble $LiAlSiO_4$ and $CaSiO_3$ [70]. CaO lowered the melting temperature, promoting structural alteration of β-spodumene and further acid leaching. For the best results, 20% CaO, a roasting temperature of 1200 °C, a holding time of 1.5 h, an H_2SO_4 concentration of 120 g/L, a L/S ratio of 7:1 mL/g, a leaching temperature of 80 °C, and a leaching time of 1.5 h were used. The Li-leaching yield was 96.18%. Li was introduced into the leaching liquid by the action of H_2SO_4 during leaching, and the primary components of the leaching residue were silicate and calcium sulfate. To begin, 30 g of spodumene concentrate powder and CaO were mixed in the required ratio and deposited in a corundum crucible before being moved to a muffle furnace. The temperature of the furnace was raised at a rate of 10 °C/min from an ambient temperature to a target temperature. When a preset temperature was reached, it was held for a specified length of time (soaking time or holding time). In the furnace, the roasted products were cooled to room temperature before being subjected to sulfuric acid leaching.

Based on the roasting results, the proposed reaction mechanism is as follows:

$$\alpha - LiAlSi_2O_6 \rightarrow \beta - LiAlSi_2O_6 \tag{23}$$

$$CaO + SiO_2 = CaSiO_3$$

$$\beta - LiAlSi_2O_6 + CaO = LiAlSiO_4 + CaSiO_3$$

The leaching yield of Li was only 13.70% without the addition of CaO. However, increasing the CaO dosage from 10% to 20% raised the leaching yield of Li from 32.04% to 90.69%, indicating that the reaction between CaO and spodumene was suitable at 20% (Figure 14b). With the increasing H_2SO_4 concentration, the leaching yield of Li (with H_2SO_4) increased until it reached a plateau at 120 g/L (a yield of 97.23%). The leaching yield of Al grew steadily across the same range of H_2SO_4 concentrations, reaching a maximum of 86.05% at an acid concentration of 150 g/L (Figure 14c). The leaching yield of Li steadily increased to 97.23% when the L/S ratio was in the range of 5:1 mL/g to 7:1 mL/g (Figure 14d). The leaching yield of Li remained essentially constant as the L/S ratio exceeded 7:1 mL/g, but the leaching yield of Al increased throughout the procedure. At a L/S ratio of 9:1 mL/g, the maximum leaching yield of Al was 99.66%, suggesting that Li and Al were virtually entirely leached.

Water-leaching studies were carried out to extract Li from β-spodumene after combining with CaO [71]. An estimated 97.2% of the Li was recovered after four cycles of water leaching (Figure 14e). An ion-exchange reaction with calcium was used to perform Li leaching. Particles of ~75 µm, a CaO-to-β-spodumene mass ratio of 3:1, pulp density (solid mass-to-liquid volume ratio) of 10%, reaction temperature of 100 °C, stirring speed of 200 rpm, and reaction duration of 9 h were the most suitable parameters. To prepare a leaching sample of CaO and β-spodumene for recursive leaching phases, the leach residue, which included $Ca(OH)_2$, $CaCO_3$, and unreacted β-spodumene, was calcined at 900 °C. Water-leaching studies were carried out in a 1–1 five-neck flask fitted with a stirrer and a heating mantle. A condenser was fitted to prevent the lixiviant from evaporating during the leaching process. The leach residue was calcined using an alumina crucible in a muffle furnace. As shown in Figure 14f, following four stages of the water-leaching reaction, 39.2%, 31.7%, 18.3%, and 8% of the Li could be leached through the 1st, 2nd, 3rd, and 4th water-leaching phases, respectively, for a cumulative yield of 97.2%.

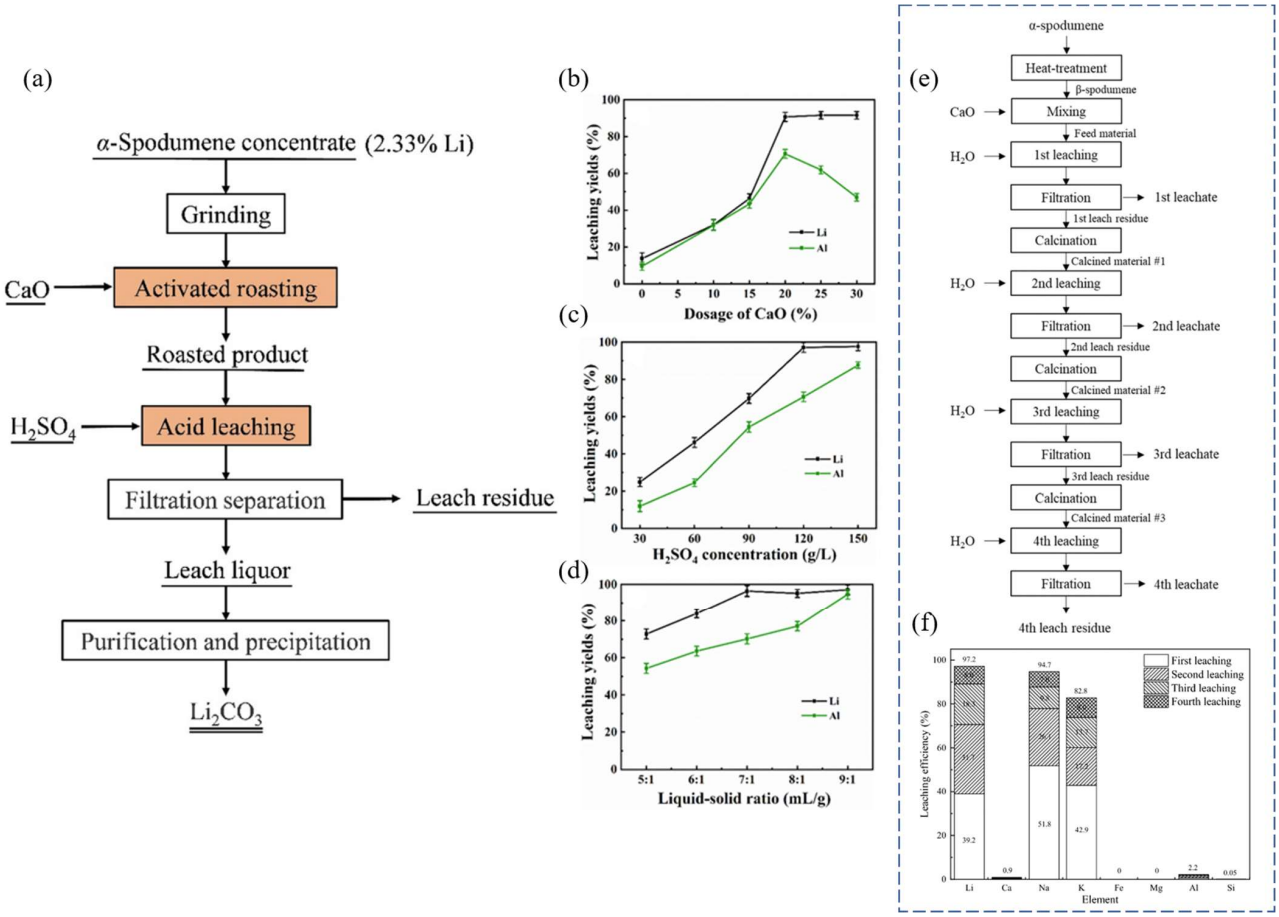

Figure 14. (**a**) Schematic of the extraction process flow for Li extracted from the α-spodumene concentration. (**b**) Effects of CaO dosage (1100 °C, 2 h) on the extraction of Li and Al. Constant leaching conditions: H_2SO_4 of 120 g/L, L/S of 7:1 mL/g, leaching temperature of 80 °C, and leaching time of 2 h. (**c**) Effect of H_2SO_4 concentration (7:1 mL/g, 80 °C, and 2 h). (**d**) L/S ratio (120 g/L H_2SO_4, 80 °C, and 2 h). For (**c**,**d**) Constant leaching conditions: roasting temperature of 1200 °C, CaO dosage of 20%, and holding time of 1.5 h. Adapted with permission from [70]. (**e**,**f**) Serial calcination and water leaching with CaO. (**e**) Flowchart for water leaching and calcination to extract Li. (**f**) Metal-ion-leaching efficiency in a four-stage experiment [71].

2.5. Sulfate Roasting

Zeelikman et al. described the roasting of α-spodumene using K_2SO_4 [72]. The reaction between spodumene and K_2SO_4 has been shown to begin at 700 °C. In reality, however, roasting is frequently performed at 920–1150 °C, when α-spodumene is first transformed into its β-phase before entering a substitution process with K_2SO_4. Furthermore, because the reaction is reversible, a substantial excess of K_2SO_4 was required in reality to ensure successful Li extraction as $LiSO_4$ [72].

Kuang et al. presented a closed-loop methodology for the recovery of Li from β-spodumene through the process of leaching with Na_2SO_4 [73]. Two types of additives: calcium oxide (CaO) and sodium hydroxide (NaOH), were utilized to improve the extraction efficiency. The reported Li extraction efficiencies were 93.30% when CaO was added and 90.70% when NaOH was added. These were achieved under the following conditions: Na_2SO_4/additive (CaO or NaOH)/ore mass ratio of 9:0.4:20, temperature of 230 °C, L/S ratio of 7.5 mL/g, particle size (D_{90}) of 39 µm, autoclaving pressure of 2.7 ± 0.1 MPa, and time of 3 h. Through the examination of the leaching residue, it was determined that the extraction mechanism involves a highly chemo-selective ion-exchange process between Li^+ in β-spodumene and Na^+ in a Na_2SO_4 solution. In the investigation, the α-spodumene

(Greenbushes, Australia) was transformed to β-spodumene by calcining it in a rotating kiln at 1100 °C for 1 h. The β-spodumene leaching was accomplished by putting the β-spodumene/Na_2SO_4 combination in a 200 mL stainless-steel autoclave. The comparative analysis of the extraction efficiency of Li was conducted by introducing either CaO or NaOH in each experimental trial, while maintaining consistent leaching conditions. The impacts of various variables on Li extraction efficiency were explored: Na_2SO_4/ore mass ratio, additive/ore mass ratio, leaching temperature, ore particle size, leaching time, and L/S ratio (Figure 15—only three shown).

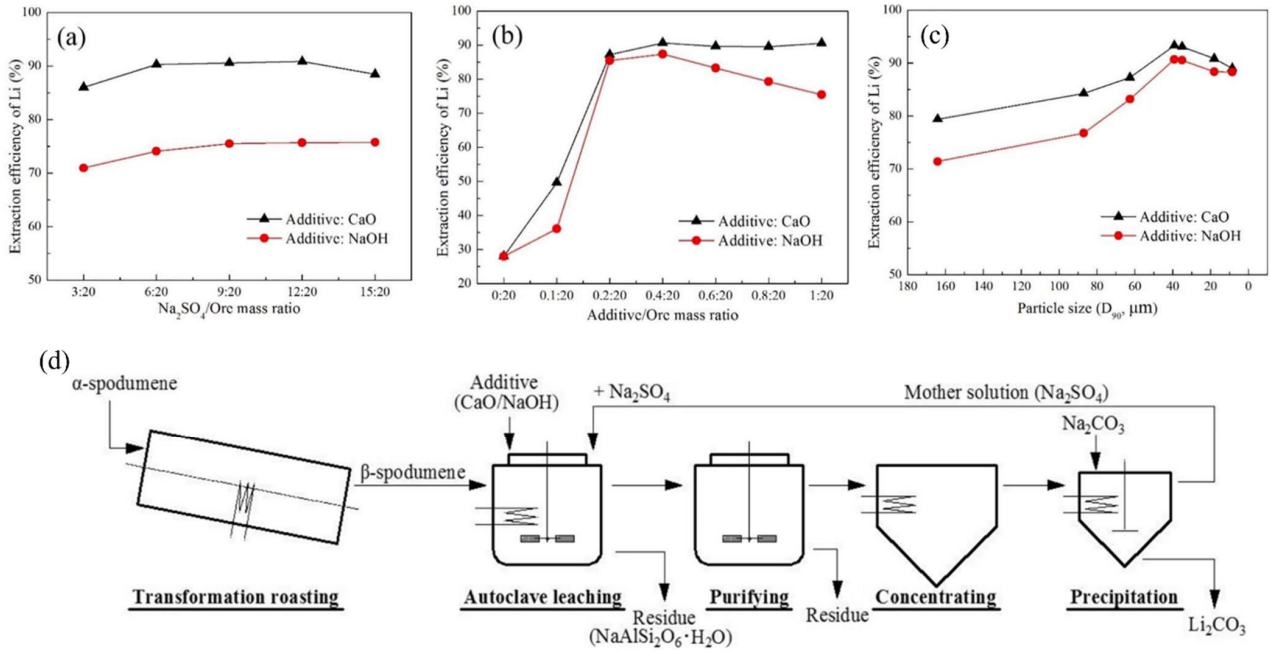

Figure 15. Effects of various factors on the Li extraction efficiency. (**a**) Na_2SO_4/ore mass ratio, (**b**) additive/ore mass ratio, and (**c**) particle size (D_{90}). (**d**) Flow diagram of the proposed closed-loop process for extracting and recovering Li from spodumene. Adapted with permission from [73].

When compared to acid approaches, the sulfate method via roasting or autoclaving can significantly minimize Al and Fe dissolution, simplifying the downstream purification process and reducing potential Li losses. The sulfate roasting technique often employs reagents: potassium sulfate and sodium sulfate. The quantities of these reagents required are substantial, ranging from around 40% to 60% [74,75]. Consequently, this poses a challenge in terms of elevated production expenses. However, the utilization of Na_2SO_4 can significantly reduce expenses associated with reagents due to its cost-effectiveness and ability to be recycled efficiently. Table 2 displays a summary of the different processes reported in the patents and literature.

Table 2. A summary of the different processes for recovering Li from spodumene that have been published in patents and studies.

Process	Experimental Conditions	End Product/Recovery %	Ref.
Acid	Roasting: ore/HF/H_2SO_4 ratio of 1:3:2 (g/mL/mL), at 100 °C for 3 h; water leaching at 50 °C	Recovery of Li: 95%	[47]
	Calcined at 1025 °C, roasting with H_2SO_4 at 175 °C; leaching with H_2O	Recovery of Li: 93%; 99.9% pure $LiOH{\cdot}H_2O$	[76]
	Roasting (1050–1090 °C) and H_2SO_4 leaching; water leaching at 225 °C	96% pure Li_2CO_3	[57]

Table 2. *Cont.*

Process	Experimental Conditions	End Product/Recovery %	Ref.
Alkaline	Roasting Na_2SO_4/CaO or NaOH as additive/β-spodumene; leaching at 230 °C	Recovery of Li: 93.3% (CaO), 90.7% (NaOH)	[73]
	Roasting with Na_2CO_3 at 550–650 °C for 30 min, followed by water leaching at RT	Recovery of Li: 92%; 98% pure Li_2CO_3	[77]
	Hydrothermal alkaline treatment at 250 °C; α-spodumene + NaOH solution	Li_2CO_3 as product; Li recovery of 95.8%	[61]
	Autoclave alkaline treatment; α-spodumene + NaOH solution; acid leaching	Li_2O extraction efficiency of 87.3%	[62]
	Autoclave alkaline treatment; α-spodumene + KOH solution	Li extraction efficiency could reach 89.9%	[63]
	Roasting (320 °C): α-spodumene + NaOH; acid leaching and water leaching; Na_2CO_3 roasting at 851 °C)	88% for NaOH; 76% for Na_2CO_3	[65]
	Roasting (1200 °C) with CaO; H_2SO_4 leaching	Leaching yield: 96.18%	[70]
Chlorination	Chlorination (using $CaCl_2$) at ~700 °C; water leaching	90.2% Li extracted as LiCl at 900 °C	[54]
	Roasting of β-spodumene with Cl_2 at 1100 °C, 150 min	LiCl extracted at 1100 °C	[20]
	Roasting (550–1200 °C, 120 min) with $MgCl_2$-$CaCl_2 \cdot 12H_2O$; leaching with H_2O, HCl	LiCl extraction efficiency 50–90%	[56]
	Roasting (1000–1050 °C, 15–60 min) with KCl, NaCl; leaching with H_2O/HCl	LiCl product; 85–97.5%	[78]
	Roasting (800–1200 °C, 180–720 min) with $CaCl_2$; leaching reagent alcohol	LiCl product; 96.5–98.5%	[79]
	Roasting (250–750 °C) with NH_4Cl; water leaching	LiCl product; 97–98%	[80]
Carbonation	Roasting (100–205 °C, 60 min) with CaO + H_2O; H_2O leaching	LiOH product; 97%	[81]
	Roasting (1000–1230 °C) with CaO + H_2O; water leaching	LiOH product; 80%	[81]
	Roasting (150–250 °C, 10–120 min) with Na_2CO_3; water leaching	Li_2CO_3 product; 94%	[69]
	Autoclaving with Na_2CO_3 at 225 °C for 60 min; water leaching	Li_2CO_3 product; 70% 94% Li was extracted from β-spodumene	[57]
Sulphation	Roasting (1000–1150 °C, 120–180 min) with $CaSO_4$ + $CaCO_3$; water leaching	Li_2SO_4 product; 85–90%	[82]
	Roasting with Na_2SO_4 + CaO; leaching at 230 °C	Li_2SO_4 product; 93.3%	[73]
	Roasting (200–300 °C) with Na_2SO_4 + NaOH; leaching with Na_2SO_4 + NaOH	Li_2SO_4 product; 90.7%	[73]
Fluorination	Roasting (600 °C) β-spodumene with NaF; leaching with HF	LiF product; 90%	[83]
	HF + H_2SO_4/α-spodumene at 100 °C, 3 h	Li: 96%	[84]

2.6. Microwave-Assisted Processing

The traditional thermal processing of α-spodumene necessitates spending a significant quantity of energy, resulting in a notable financial impact on the overall expense of Li extraction. The microwave (MW) heating as a possibly less energy-intensive alternative has been explored for different applications for several decades [85,86]. The process of heating materials conventionally involves the transfer of heat from the exterior of a body toward its interior through conduction, convection, and radiation methods. MWs possess the ability to permeate a wide range of nonmetallic substances, hence offering the distinct advantage of volumetric heating [87]. MW is an electromagnetic radiation

characterized by frequencies ranging from 300 MHz to 300 GHz (Figure 16a). In the industrial and commercial sectors, the frequencies of 915 MHz and 2450 MHz are widely employed for various applications. The heating mechanism of MWs is contingent upon the dielectric characteristics displayed by the constituent components. Selective heating occurs when a material comprises more than one component with very varied dielectric characteristics. This selective heating, together with the thermal characteristics of the material components, usually determines whether MW heating offers any advantages over traditional heating. The utilization of MWs in heating processes offers significant advantages in terms of volumetric and selective heating, resulting in a substantial reduction in heating periods compared to conventional heating methods, frequently by less than 1%. Reduced treatment durations also facilitate substantial downsizing of equipment. Hence, MWs can be effectively utilized in specific applications. To harness this potential, it is imperative to use a multi-disciplinary approach. This entails acquiring a comprehensive comprehension of MW heating mechanisms, electromagnetic field patterns, dielectric properties of materials, and the specific industrial process at hand. This knowledge is indispensable in the development of efficient MW equipment [87].

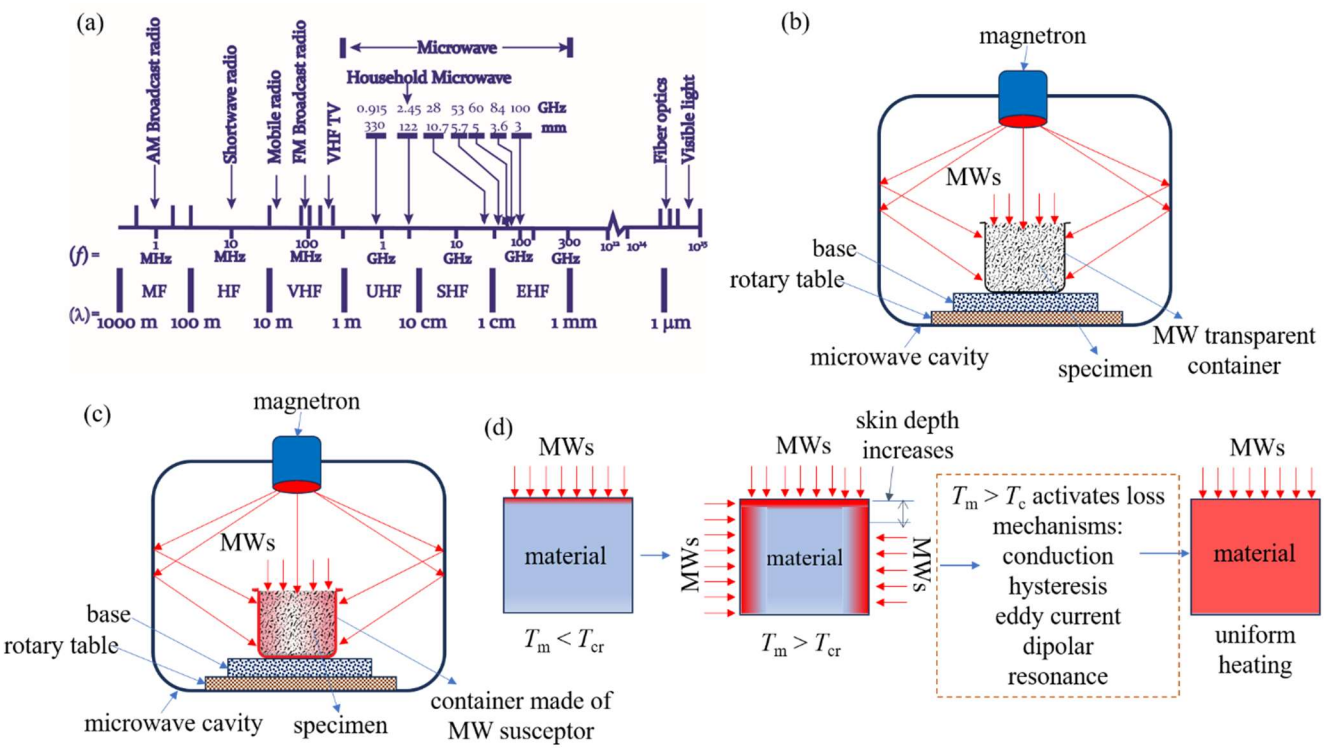

Figure 16. (**a**) Segment of the MW region in the electromagnetic spectrum. (**b**) Direct MW heating without a susceptor in a multimode MW applicator. (**c**) Hybrid heating with a MW-absorbing specimen holder. (**d**) MW absorption and heating mechanism when the material temperature reaches the critical temperature (T_{cr}) of a material.

2.6.1. MW Heating Mechanisms

Materials can be categorized into three classes based on the mechanism of MW's interaction with them: insulators, conductors, and absorbers. MWs are absorbed by most carbon-based materials. Insulating materials, such as quartz or PTFE, are MW-transparent. MWs can be reflected by conductors, such as aluminum or stainless steel. A thorough examination of electromagnetic wave interaction and absorption in liquids and solids is beyond the scope of this article and can be found in articles published previously [87]. Dielectrics are materials that can absorb high-frequency electromagnetic waves and heat in a number of ways. The primary heating mechanisms in the industrial high-frequency heating range (10^7 to 3×10^9 Hz), which includes radiofrequency and MWs,

comprise dipolar polarization, conduction, and interfacial polarization. The conduction mechanism arises due to the presence of a restricted number of free charges inside the material matrix, such as in graphite. This mechanism typically remains rather consistent at low MW frequencies but diminishes as the frequency increases, reaching a point of decline at about 100 MHz. The material exhibits low electrical conductivity, and the flow of unbound charges leads to thermal energy generation due to electrical resistance. The dipolar polarization mechanism is a result of the presence of molecules in the dielectric material that possess a dipole moment. Under the influence of an externally imposed electric field, the dipoles orient themselves in alignment with the direction of the field. When subjected to a varying electric field in the presence of MW radiation, the dipoles within the dielectric material undergo oscillations, resulting in an augmentation of the internal energy of the dielectric material. The dissipation of internal energy through friction might result in the thermal elevation of the material. Interfacial polarization, also known as Maxwell–Wagner polarization, pertains to the accumulation of charged particles at interfaces inside heterogeneous dielectric materials. The mechanism by which a dielectric material absorbs MWs and transforms them into thermal energy can be elucidated through the utilization of the complex permittivity (ε^*). In this context, the real component of the complex permittivity represents the dielectric constant (ε'), while the imaginary component corresponds to the dielectric loss (ε''). This relationship is represented as $\varepsilon^* = \varepsilon' - j\varepsilon''$.

The dielectric constant expresses a substance's ability to store electromagnetic energy through its charges and dipoles. The dielectric loss factor measures a dielectric's ability to dissipate internal energy trapped in the material as heat. The dielectric loss factor-to-dielectric constant ratio evaluates a material's ability to absorb electromagnetic energy and dissipate it as heat throughout the substance. The parameter known as the dissipation factor or loss tangent, $\tan\delta = \varepsilon''/\varepsilon'$, is frequently employed to define a material's heat absorption capability in an externally applied electromagnetic field [88]. Many inorganic materials are known to strongly couple (interact) with MWs at room temperature. Table 3 includes several of these minerals and inorganic compounds. The table also includes the temperatures obtained by these materials and the accompanying exposure times when irradiated by MWs in standard residential MW ovens.

Table 3. MW-active elements, natural minerals, and compounds [88].

Element/Mineral/ Compound	Time (min) of MW Exposure	*T*(K)	Element/Mineral/ Compound	Time (min) of MW Exposure	*T*(K)
Al	6	850	NiO	6.25	1578
C (amorphous, <1 µm)	1	1556	V_2O_5	11	987
C (graphite, 200 mesh)	6	1053	WO_3	6	1543
C (graphite, <1 µm)	1.75	1346	Ag_2S	5.25	925
Co	3	970	Cu_2S (chalcocite)	7	1019
Fe	7	1041	$CuFeS_2$ (chalcopyrite)	1	1193
Mo	4	933	$Fe_{1-x}S$ (phyrrhotite)	1.75	1159
V	1	830	FeS_2 (pyrite)	6.75	1292
W	6.25	963	MoS_2	7	1379
Zn	3	854	PbS	1.25	1297
TiB_2	7	1116	PbS (galena)	7	956
Co_2O_3	3	1563	CuBr	11	995
CuO	6.25	1285	CuCl	13	892
Fe_3O_4 (magnetite)	2.75	1531	$ZnBr_2$	7	847
MnO_2	6	1560	$ZnCl_2$	7	882

It should be noted that all materials do not couple with either the electric field or magnetic field equally. Some materials may absorb the *E*-field of MWs more than the *H*-field. Hence, it is important to thoroughly analyze the dielectric characteristics of the material under various processing settings in order to effectively plan MW experiments and develop industrial MW equipment. If the material is not absorbing the *E*-field or *H*-field, it is possible to heat the material indirectly using a material called a susceptor, which can function as a heat source. A susceptor is a material with a high dielectric tanδ. This substance has the ability to absorb electromagnetic energy and convert it to heat. A susceptor may keep in contact with the sample. Alternatively, a sample can be stored separately by surrounding the reaction vessel (or test tube) in a susceptor material container, or the sample may be kept in a material made of a susceptor (Figure 16c). Carbon (graphite or amorphous carbon), copper (II) oxide, and SiC are common susceptors. The use of a susceptor (direct contact with a sample) can lead to complications. For example, reactions involving a combination of susceptors and reagents may result in product contamination (or even undesirable side reactions), necessitating an additional separation step in the synthesis process. As we will see in the following section, α-spodumene has been found to not directly absorb MWs. However, using a susceptor, it is possible to deliver energy to it via indirect (hybrid) heating. It is important to note that many semiconductors, metals, and alloys do not absorb MWs when they are in bulk form. However, when the size of their particles is reduced, they absorb MW energy and aid in the uniform heating of the sample [87].

2.6.2. Microwave-Assisted Decrepitation and Li Extraction

It has been discovered that microwave energy has the potential to be used in a variety of mineral treatment and metal recovery procedures, including smelting, roasting, and heating [89–92]. Peltosaari et al. investigated the technical potential for generating heat for the conversion process of spodumene concentrate (7.2% Li_2O) using MWs [16]. The heat treatment experiments were conducted using a household MW furnace with a power output of 700 W.

A SiC susceptor was employed in the MW furnace (Figure 17a), while a conventional resistance-heated furnace was used as a comparison. The phase transformation of spodumene commenced in the MW oven at a heating duration of 110 s, with the samples undergoing near-complete conversion to β-spodumene after 170 s. Evidence of partial melting of gangue minerals was discovered in the samples after a heating duration of 170 s. The duration of heating in the MW furnace for 170 s was found to be equivalent to the heating duration of roughly 480–600 s at a temperature of 1100 °C in the conventional furnace. Furthermore, apart from the α- and β-forms, an intermediate phase, known as hexagonal γ-spodumene, was observed in samples subjected to heating using both furnaces. In the experiment, pegmatitic spodumene was crushed and then sieved into different particle size samples. The conversion rate of spodumene was not found to be significantly influenced by particle size in the limited sample size employed in this investigation. It was speculated that the direct heating of the samples by MWs did not occur, and instead, the heating was solely facilitated through conduction and radiation originating from a heated SiC tube. A minute quantity of γ-spodumene was observed to be generated during hybrid MW studies, following 110 s of heating at a temperature of 910 °C. In the context of traditional furnace studies, it was seen that γ-spodumene materialized at a temperature of 800 °C and underwent a complete transformation into β-spodumene after being subjected to a heating duration of 900 s at 1100 °C. As shown in Figure 17b, during the first 140 s, the finest 0.5–0.85 mm fraction converted slightly faster than coarser fractions, and the 1.0–2.0 mm fraction slightly slower than other fractions. However, there was no difference at the end of heating.

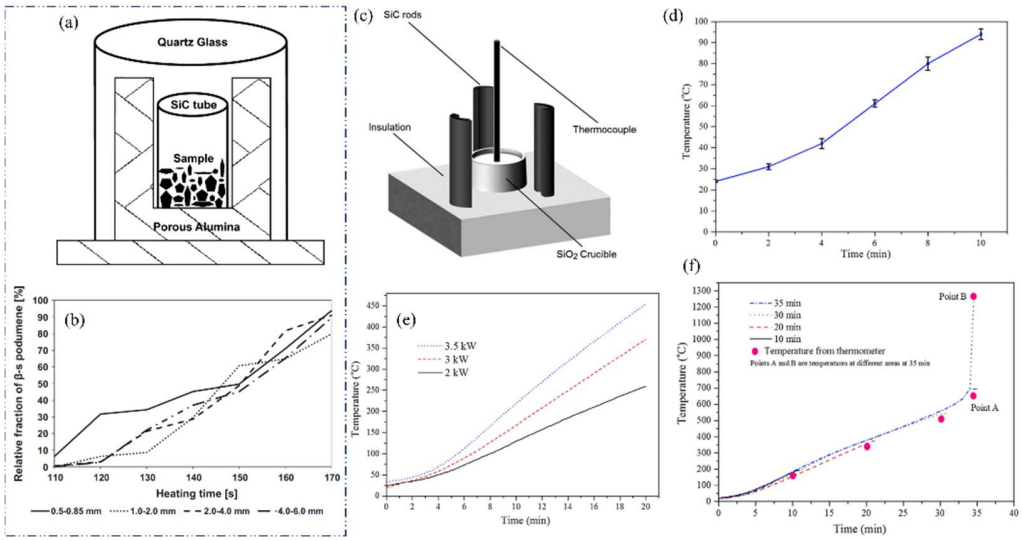

Figure 17. (**a**) Schematic diagram of sample, susceptor, and thermal insulation for MW heating. (**b**) Relative fractions of β-spodumenes in the samples after MW heating [16]. (**c**) Schematic of the MW calcination setup: (1) SiO_2 crucible, (2) SiC rods, (3) thermocouple, and (4) insulation. (**d**) Temperature of spodumene concentrate microwaved at 3 kW for 10 min without a susceptor. (**e**) Temperature profiles from hybrid MW heating (for 20 min) at different power levels. (**f**) Temperature profile from 3 kW hybrid MW heating at various time durations [93].

Although MW irradiation has advantages over traditional heating methods, one major drawback is that not all minerals respond to MW irradiation. Some materials, notably spodumene, cannot be MW-heated successfully at RT because they do not absorb MWs at that temperature. At RT, silicates in general have been claimed to be transparent to MW energy. However, once these materials reach a particular temperature, known as the critical temperature (T_{cr}), they can transform into MW absorbers. This process is depicted in Figure 16d. In some circumstances, this natural feature of materials can be used to create a viable MW treatment of such minerals by preheating them using traditional heating methods. When these minerals reach temperatures over the T_{cr}, they begin to heat up significantly faster by absorbing MWs. At this temperature, a single dominant process or a combination of different processes may contribute to uniform heating (Figure 16d).

Experimentally, it has been shown that the T_{cr} for α-spodumene concentrate is found to be approximately 634 °C [93]. In the experiment, spodumene concentrate was heated using (i) direct and (ii) hybrid MW methods. According to the findings, spodumene concentrate is transparent to direct MW irradiation. However, utilizing hybrid heating to preheat the sample, it was discovered that once heated to above 634 °C, α-spodumene irradiated with MWs undergoes rapid localized conversion into γ- and β-spodumene, forming a β-spodumene product in either sintered or molten form in a matter of seconds. Energy input calculations revealed that the energy required to make the sintered product could be significantly less than the energy required to convert α- to γ- and β-spodumene in a muffle furnace. In each instance of conducting a standard test, a representative sample weighing 20 g of spodumene concentrate was carefully deposited into a quartz (SiO_2) crucible. The crucible measured 60 mm in diameter and 50 mm in height. The SiO_2 is MW transparent, hence avoiding any interference with the MW heating process. To establish a conducive setting for hybrid heating, three silicon carbide (SiC) rods (measuring 40 mm in width and 100 mm in height) were strategically positioned around the crucible, as depicted in Figure 17c. The adjustable power range of the MW furnace (frequency 2.45 $\pm$ 0.05 GHz) ranged from 0.1 to 6.0 kW, with a recommended working power of 3 kW. Figure 17d depicts the variation in temperature of the spodumene concentrate sample when subjected to a MW power of 3 kW for a duration of 10 min, without the inclusion of silicon carbide (SiC) rods. The findings indicate that the temperature of the spodumene concentrate did not exceed

95 °C. The temperature profiles obtained via hybrid MW heating at various power settings for a duration of 20 min are depicted in Figure 17e. The experimental results indicate that the final temperatures achieved were around 370 °C when the power setting was 3 kW, and 450 °C when the power setting was increased to 3.5 kW.

Figure 17f displays the temperature profiles obtained from four distinct experiments conducted in the hybrid heating setup, each with varying durations ranging from 10 to 35 min (under the operation of a 3 kW MW power set). The findings indicate that after an initial period of reduced heating, the temperature of each sample exhibited a consistent and steady increase of 20 °C/min, until reaching around 634 °C, which occurred at the 32 min mark. The temperature measurements of the samples obtained at time intervals of 10, 20, and 30 min showed a high degree of consistency across various locations within each sample. Furthermore, the visual characteristics of the samples indicated that they possessed a homogenous composition. However, a notable alteration in this pattern was noted at the 32 min mark, namely, when the temperature had reached 634 °C. Initially, it was seen that there was a significant disparity in the temperature across various sections of the sample, suggesting a distinct reaction to the heat generated throughout the experiment. The recorded temperatures within various regions of the sample exhibited a range spanning from 650 °C to 1270 °C. This observation suggests that specific sections of the sample had a temperature rise of ~200 °C/min, signifying a ten-fold augmentation in the heating rate. The low- and high-temperature extremes observed in the experiment are denoted as point 'A' and point 'B' in Figure 17f. Considerable diversity was also noted in the physical characteristics of the sample generated after 35 min.

The occurrence of a more rapid temperature increase over 634 °C, as depicted in Figure 17f during the final minutes of the 35 min experiment, can be attributed to a thermal runaway phenomenon. This phenomenon may indicate the initiation of MW energy absorption by the sample.

The same author employed MW ovens for the acid roasting of β-spodumene to facilitate Li extraction, and afterwards conducted a comparative analysis with conventional furnace heating [94]. In this experiment, MWs were employed to assess their effectiveness on Li extraction via acid roasting of β-spodumene, rather than to convert it to α-spodumene. In the presence of 80% excess concentrated H_2SO_4, traditional acid roasting of 5 g of β-spodumene at 250 °C for 60 min was highly effective in Li extraction. The MW technique, on the other hand, recovered almost all the Li after only 20 s of irradiation. The grinding of the spodumene sample resulted in a reduction of the excess acid required for achieving nearly full recovery of Li to 15%. Li extraction was reduced following MW irradiation of the sample for more than 20 s, with the lowest value being 42% after 240 s. The use of MWs was found to be energy-efficient. The typical muffle furnace heating method consumed 10.4 MJ of energy, which was much higher than the MW energy of 15.4 kJ necessary to extract the same percentage of Li from β-spodumene. β-spodumene, which was used in the heating experiments, was synthesized by calcination of α-spodumene at 1100 °C for 2 h and then used for conventional and MW-assisted acid roasting. Figure 18b shows the measured temperature of samples vs. the MW exposure time and, as indicated, the temperature of the sample under MW irradiation rose from 260 °C to 690 °C when the time was extended from 10 to 240 s. Figure 18c depicts the Li extraction following water leaching for various heating durations. A heating duration of 20 s resulted in nearly full Li extraction. The results for β-spodumene treated with 15 and 80% excess acid, as well as pulverized β-spodumene (mortar and pestle for a minute) treated with 5%, 10%, and 15% excess acid, are shown in Figure 18d. Li extraction was ~99% during MW roasting of the ground sample with 15% excess acid.

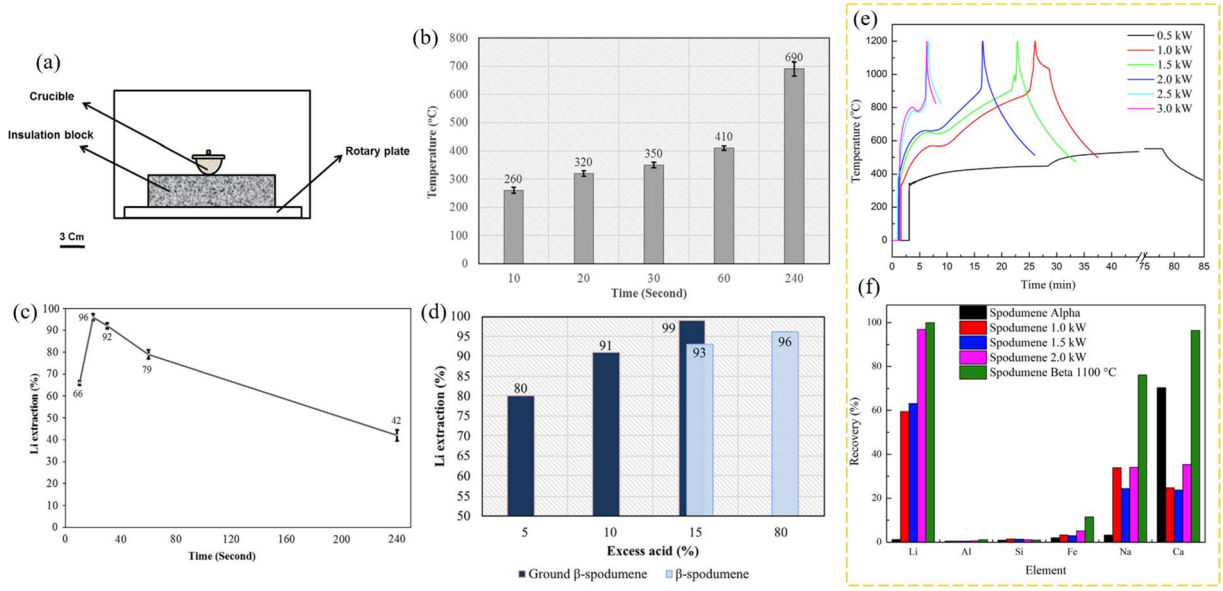

Figure 18. (**a**–**d**) Acid roasting of β-spodumene: MWs vs. conventional heating. (**a**) Schematic design of MW setup with a ceramic crucible, with sample and an alumina insulating block. (**b**) Measured temperatures of samples after 10, 20, 30, 60, and 240 s of MW exposure. (**c**) Extraction (water leaching) of Li following MW acid roasting of β-spodumene for 10, 20, 30, 60, and 240 s. (**d**) Effect of excess acid on Li extraction from β-spodumene and ground β-spodumene samples after exposure to MW for 20 s [94]. (**e**,**f**) MW-assisted calcination of spodumene. (**e**) Temperature profiles of spodumene measured at various MW strengths (0.5 kW to 3 kW). (**f**) A comparative analysis of leaching recovery of major elements from spodumene calcined via MW and conventional heating techniques [95].

During MW-assisted calcination, the effects of MW power on the phase transformation, structural changes, and leachability of spodumene were studied and compared with that of conventional heating [95]. The results revealed that at 2.0 kW MW power, the optimum Li recovery by the MW calcination–acid roasting–leaching process reached 97%, which is comparable to traditional heating. The spodumene MW temperature profiles and characterization data revealed that α-spodumene began to transition into γ- and β-spodumene at about 900 °C. The T_{cr} for α-spodumene observed in this investigation under 1.0–2.0 kW MW power was in the range of 570–660 °C. MW heating also resulted in decreased Fe, Na, and Ca recovery values in the leaching process. The spodumene concentrate consisted of 92% spodumene and 8% quartz, and a multimode cavity MW chamber was employed. In a typical furnace, a baseline calcination experiment was performed to compare the outcomes of totally converted spodumene concentrate into β-spodumene using conventional heating to the results of MW trials. For each test, 5 g of spodumene concentrate was deposited in an alumina crucible (32 mm diameter and 35 mm height). Six SiC rods (12 mm diameter and 27 mm height) were put around the crucible as susceptors for hybrid heating. To explore the efficacy of MW calcination on spodumene concentrate, a series of calcination experiments were performed using different power levels, ranging from 0.5 to 3.0 kW, with an increase of 0.5 kW. Figure 18e displays the profiles of temperature vs. MW power for the given samples. At a MW power of 1.0 kW, the sample's peak temperature may exceed 1200 °C within a 30 min duration. However, at a power of 2.5 kW or more, the peak temperature could be achieved in less than 10 min. To extract Li from the calcined samples, a standard procedure involving acid roasting of β-spodumene followed by water leaching was employed. Figure 18f illustrates the leaching recovery of key components. The findings of the preceding research show that the transformation of α-spodumene by MW calcination is comparable to the conventional procedure, with less energy spending.

With the aim of decrepitation, α-spodumene was subjected to MW irradiation, and then the mineral underwent sulfuric acid decomposition [96]. In the investigation, the

mineral was crushed to various sizes (1.0, 0.5, and 0.25 mm). The heating procedure was used on samples of various sizes until a temperature of 1200 °C was achieved. Sulfation of calcined materials was carried out for 60 min at 250 °C. After cooling to 22 °C, distilled water was added and mixed in closed leaching vessels for 120 min. The recovery of Li following MW exposure and leaching was reported to be 96.82% for particles smaller than 0.25 mm. MW heating resulted in the lower recovery rates of Fe, Na, and Ca in the leaching process.

2.7. Mechanical Activation

Metal extraction from minerals has traditionally involved an initial size reduction process on the ore. As a result, the liberation of the various mineral particles is aided. Size reduction is particularly crucial in the subsequent chemical processes for increasing the surface area and boosting the accessibility of the precious mineral to reagents (e.g., the leachant) [97]. Mechanical activation is one of the most important pre-treatment procedures that influence the leachability of the solid phase in this context. This approach provides for a reduction in the temperature of mineral decomposition or creates enough disordering that thermal activation can be avoided entirely. In addition to a particle size reduction, the material may undergo phase shifts due to high local pressures and temperatures at the particle contact locations, as well as defects in the material. According to Alex et al. [98], mechanical activation causes the surface area to expand in either a reversible or irreversible fashion (surface activation), and the crystal structure to become unstable (lattice or bulk activation). Furthermore, the system's state change reduces the crystals' coherence energy or the atoms' binding energy in solids, resulting in a structural modification. These changes, which are related to an increase in the system's free energy, increase reactivity and correspond to the particles being mechanically activated. The complicated influence of surface and bulk characteristics occurs throughout this process. Mineral activation has a beneficial effect on the kinetics of the leaching reaction, as well as a rise in surface area and other phenomena. Activation can be conducted either in air or in a suitable liquid medium. Studies have shown that mechanical activation increased the reactivity of the Li mineral, lepidolite (which has a layered structure) [99].

Kotsupalo et al. [99] explored the mechanical activation of α-spodumene in both air and water, with the goal of converting it to a more reactive phase, and found that it improved Li extraction. Mechanical activation of α-spodumene in centrifugal planetary apparatuses altered the mineral's structure and resulted in the cleavage of the Me-O (Me-Li, Al) bonds. Further acid and alkali treatment resulted in a nearly complete migration of aluminum and Li to the liquid phase. The alkaline breakdown of activated spodumene produced aluminate solutions, from which lithium aluminum hydroxide $LiOH{\cdot}2Al(OH)_3{\cdot}mH_2O$ was precipitated [99]. Vieceli et al. demonstrated that mechanical activation causes lepidolite amorphization and, as a result, increased reactivity via sulfuric acid digestion and water leaching. Necke et al. demonstrated that petalite is far more appropriate for the alkaline mechanochemical method than spodumene or lepidolite, with 84.9% Li extraction and nearly full conversion to hydrosodalite after 120 min of ball milling in alkaline media. The greater reactivity under these conditions can be attributed to petalite crystal structural properties, such as less dense packing and the activation of cleavage planes along Li sites during ball milling [100]. Gasalla et al. [101] explored the effect of mechanical activation on α-spodumene (Argentina). Milling for 15 min reduced the particle size from 370 to 15 µm. Longer milling times resulted in no additional particle size decrease, and fine particle aggregation was detected. According to XRD analysis of the milling results, mechanical activation not only reduced the particle size but also the crystal size. After 5 min of milling, crystals > 0.2 µm reduced to 360 Å, and after 10 min, they decreased to 200 Å. Additional grinding resulted in no additional drop in crystal size. The reduction in crystal size reduces the crystallinity of the sample, which is strongly related to amorphization. Mechanical activation's effect on β-spodumene has also been studied. Mechanical activation

of β-spodumene yields an amorphous phase comparable to mechanical activation of α-spodumene [102].

Li extraction by mechanical activation of α-spodumene with NaF and subsequent leaching with NaF/H2SO solution yielded a Li extraction efficiency of 81% at temperatures of $\leq$90 °C [103]. The milling time, temperature, leaching time, and the interaction of the latter two were found to have a positive effect on Li extraction, and the optimal conditions were a temperature of 90 °C, leaching time of 240 min, and a milling time of 600 min. During leaching, compounds Na_3AlF_6 and Na_2SiF_6 were formed, facilitating the Al and Si recovery (Figure 19d).

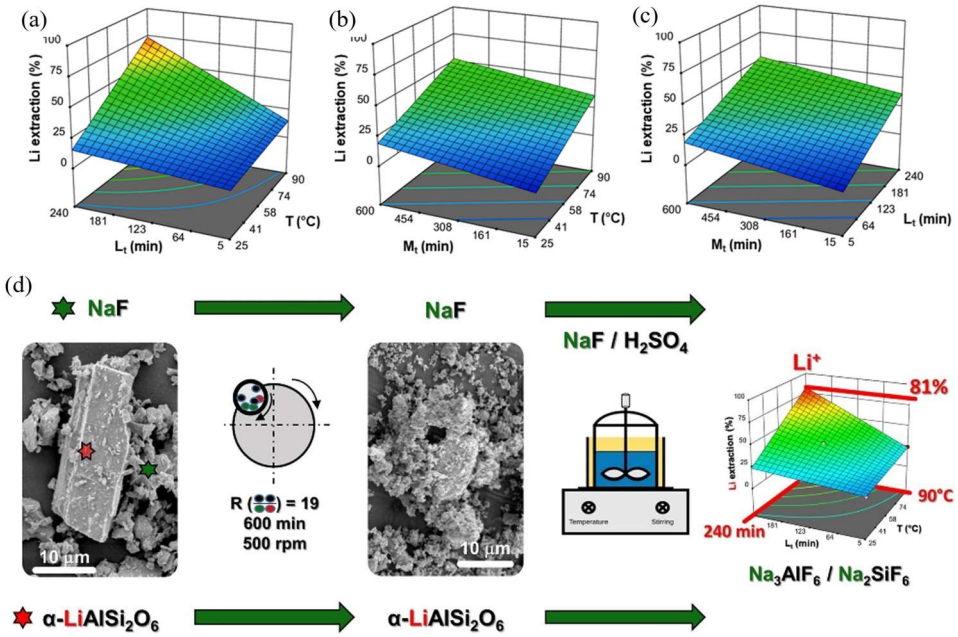

Figure 19. Mechanical activation with α-spodumene/NaF. Li extraction efficiency as a function of (**a**) leaching time (L_t) and temperature (T), (**b**) milling time (M_t) and temperature (T), and (**c**) M_t and L_t, (**d**) experimental steps for mechanical activation of the α-spodumene/NaF samples. Adapted with permission from [103].

As shown in Figure 19a, the interaction between the leaching temperature and the leaching time had a positive joint effect on Li extraction. This is because increasing the temperature promoted the synthesis of HF acid, resulting in a higher concentration in less time. Figure 19b,c indicate that Li extraction increased as the milling time increased. As the mechanical activation period increased, the mineral's crystallite size dropped, and structural deformation increased. These changes resulted in increased solid reactivity, as well as improved Li extraction.

3. Recycling Lithium and Other Precious Metals from Spent LIBs

Recycling discarded LIBs is fundamental to ecological long-term sustainability, resource conservation, and electronic waste reduction. LIBs, which are commonly utilized in electronics, renewable energy storage systems, and electric vehicles, contain valuable metals, such as Li, Ni, Co, and others. When used improperly, spent batteries may release harmful materials into soil and water, endangering both human health and the ecosystem. Recycling guarantees that these hazardous items are treated and disposed of properly, avoiding contamination and pollution [104,105]. Recycling also promotes the growth of a circular economy, which reduces waste and maximizes the use of resources. Further, recycling contributes to the recovery of these resources, reducing the burden on natural reserves and lowering mining's environmental impact. The recycling operation starts with collecting and safely disassembling spent batteries, then separating components, including

anodes, cathodes, electrolytes, and separators. These components undergo a number of steps to extract and purify the important metals.

The extraction technique usually relies on the target metal's separation. The most widely utilized approaches are hydrometallurgy, pyrometallurgy, and combined pyro- and hydrometallurgical methods [106–109]. Using chemical solutions, hydrometallurgical processes extract the metals from battery components and purify the resultant high-purity metals. Pyrometallurgical processes include melting the battery components at high temperatures. During the pre-treatment stage of the combined pyro- and hydro-metallurgical process, metals such as Li, Ni, Co, and Mn are converted into corresponding metal sulfates, carbonates, or nitrates through techniques such as sulfuric acid roasting, nitric roasting, and carbothermal reduction roasting [110–112]. These metals can subsequently be separated and extracted using water immersion, acid leaching, and other extraction techniques. The lifespan of the materials can be completed by using the extracted and purified metals to fabricate new batteries or other components. This approach enforces less demand for raw materials, promotes energy conservation, and reduces greenhouse gas emissions from mining and manufacturing operations [113].

Ding et al. used in situ thermal reduction to achieve the simultaneous removal of organic matter, reduction of high-valence-transition metals, and dissociation of spent LIB electrode materials, all of which are important steps toward the hierarchical selective recovery of precious metals [114]. This method involves a combination method for the progressive recovery of precious metals, which included in situ thermal reduction, ultrasonic-assisted water leaching, wet magnetic separation, and sulfuric acid leaching from a powdered mixture of cathode and anode materials. It was discovered that spent cathode materials were decomposed and synchronously reduced to NiO, MnO, Ni, LiF, Co, $LiAlO_2$, Li_2O, and Li_2CO_3 by in situ thermal reduction after 1 h of roasting at 650 °C. The maximal Li-leaching efficiency under standard water-leaching conditions was determined to be 85.66%. Ultrasonic-assisted leaching has been found to cause ultrasonic cavitation effects in the leaching process, enabling the dissolution and desorption of LiF, Li_2CO_3, and Li_2O by mechanical action and thermal effects at the solid–liquid interface, resulting in a 98.68% Li-leaching efficiency. The retrieved leaching solution was evaporated and crystallized, yielding high-purity Li_2CO_3 ($\geq$99.5%). The transition metals were subsequently separated from Al, Cu, and graphite by wet magnetic separation. For detailed information on the extraction of Li and other valuable metals from waste LIBs using different techniques, readers are advised to refer to recently published articles [105,115–126].

4. Summary, Challenges, and Outlook

This review presented an overview of the methodologies currently utilized and recent laboratory-researched techniques reported on the extraction of Li from spodumene. Spodumene, a prominent Li-bearing mineral, serves as the primary source for Li extraction. Natural α-spodumene processing is the most difficult of all known Li-bearing minerals because it is inert to typical acidic and caustic treatments. The conversion of α-spodumene to a leachable phase, known as β-spodumene, entails a highly energy-intensive procedure. For several decades, decrepitation and subsequent Li extraction via techniques—acidic, alkali, chlorination, carbonation, and lime-processing methods—have been the common approaches. Li removal from spodumene can be separated into two groups: Li removal from α-spodumene without pre-treatment and Li removal from leachable β-spodumene after α-spodumene breakdown to β-spodumene. The excessive expenses of these traditional processes in terms of equipment, energy, chemicals, and environmental issues necessitate the development of new cost-effective methods.

With its high yield, the sulfuric acid method is the most extensively used industrial spodumene Li extraction technology and requires spodumene concentrate, sulfuric acid, sodium hydroxide, calcium hydroxide, sodium carbonate, and water as raw materials. The sulfuric acid method consumes considerable amounts of energy. The alkaline approach streamlines the Li-leaching and impurity removal procedures, reduces chemical

raw material and energy consumption, and reduces pollutants. Additionally, the purified solution is useful for lithium hydroxide evaporation and crystallization, as well as lithium carbonate precipitation.

Instead of sulfuric acid, the sulfate technique uses less corrosive sulfate. Due to the enormous material flow and high reaction temperature, this process takes more energy than the sulfuric acid approach. In chlorination methods, reagents can directly react with lithium ores, resulting in reduced energy consumption and a notable increase in the recovery rate of Li. However, the chlorinating technique necessitates the use of equipment that is resistant to corrosion. Autoclaving with carbonates, sulfates, hydroxides, and chlorides, for example, requires a significant amount of energy. It can, however, minimize the quantity of impurities in pregnant leaching solution. The use of hydroxides may facilitate the direct production of high-purity LiOH. During the pressure-assisted autoclaving method, additives are added to enhance the leaching efficiency of Li. However, it is apparent that the process does not induce any microstructural changes in the spodumene grains. This aspect needs further investigation. Water leaching generally demands a considerable amount of water. Techniques of purifying after leaching must be developed.

The key mechanism in fluorine-based approaches is the breakdown of Si-O bonds in silicate minerals by energetic HF molecules. As we noted earlier, fluorine-based techniques that use HF directly can achieve excellent extraction efficiency at low temperatures. For example, 90% Li can be extracted from β-spodumene in 20 min using HF at 75 °C, and 96% can be removed from α-spodumene directly (i.e., without using β-spodumene; Table 2). In terms of energy usage, fluorine-based processes outperform other methods, such as the H_2SO_4 method, roasting methods, and pressure-assisted autoclaving methods. However, the primary concerns of employing these methods revolve around issues of safety during the operation and environmental concerns, particularly in cases where HF is employed directly. Another concern is the generation of F-containing waste, which may require extra steps and additional costs for its removal.

As we observed from several studies, different forms of Li salt were obtained from spodumene: Li_2CO_3, LiOH, LiCl, and LiF. Li_2CO_3 has been extensively documented as the predominant end product, and it can be made to react with $Ca(OH)_2$ to produce LiOH, which is identified as a desirable form of Li salt for high-energy-density batteries. However, direct LiOH synthesis from spodumene is thought to be a simpler and less expensive approach. Spodumene alone does not absorb MW energy directly and efficiently. To deliver MW energy to decrepit α-spodumene, hybrid MW heating is needed. Once the ore temperature reaches the T_{cr}, the material starts to absorb MW energy rapidly, and decrepitation starts. Yet, the limitations on the amount of material that can be used for such treatment must be determined. Although this technique offers a short operation duration and is energy-efficient, the design of the customized equipment and its feasibility for processing are still unknown. More investigation is needed to understand how this technique can be scaled up to cater for large-scale samples. To improve the MW coupling with large samples, a suitable design of a reaction vessel is needed. Further, there is a need to unravel mechanisms that are prominent and facilitate absorbing the MWs from spodumene.

In mechanochemical activation-assisted Li recovery, extended ball milling of spodumene did not produce greater Li than shorter ball-milling times. The exact reason for this occurrence must be investigated. Is this pattern related to the formation of an amorphous material that somehow inhibits the Li release into the leaching solution? This needs further study. Recycling LIB is crucial for ensuring the sustainability of LIB technology. LIB recycling includes eliminating organic and iron material, separating cathode and anode materials, leaching electrodes, and recovering valuable metals from solutions through solvent extraction, ion exchange, and precipitation. The hydrometallurgical techniques used in LIB recycling may produce fluoride-containing wastewater that is difficult to handle and can contaminate the environment as a result of insufficient recycling of the organic binder and electrolyte.

Many research groups throughout the world are working on developing a futuristic battery with a very high specific capacity, the ability to run over thousands of charge/discharge cycles, extreme safety, low production costs, and low recycling costs. The importance of Li and its compounds is demonstrated by the large number of patent applications that have been filed recently targeting the recovery of Li from spodumene or other Li-bearing minerals [48,127–145]. In the following 5–10 years, other emerging batteries, such as solid-state batteries, lithium-sulfur batteries, cobalt-free lithium-ion batteries, sodium-ion batteries, iron-air batteries, zinc-based batteries, graphene batteries, vanadium flow batteries, etc., may start to partly substitute LIBs, alleviating the burden on the Li supply chain. However, LIB technology is well entrenched and holds a significant share of the energy storage market. Furthermore, Li-mining businesses around the world have made significant investments and continue to play an important role in LIB technology supply chains and other industrial uses. To make the Li recovery more economical, the same industries may recover other valuable rare earth elements from the mining wastes. Such elements can benefit many critical technologies.

Economic benefits with respect to the amount of extracted Li are a deterministic factor in evaluating the feasibility of any approach, along with its associated environmental footprint. Therefore, the process of extracting Li from spodumene should have a beneficial technology, decrease processing steps, conserve energy, boost the recovery rate of Li and other byproducts to reduce environmental effects, and improve process economy. There are benefits and opportunities for improvement in a number of present commercial technologies for extracting Li. Therefore, it is important to improve them and make them more energy-efficient, environmentally friendly, cost-effective, and easy to implement. An alternative involves direct Li extraction from spodumene. However, the timeframe of commercialization of this approach is questionable. Similarly, many laboratory-researched techniques have the potential to be commercially viable, provided their shortcomings are addressed. When implementing any processing procedure, it is integral to adhere strictly to the principles of green chemistry.

Author Contributions: Conceptualization, N.N.; methodology, N.N.; software, N.N. and R.K.C.; validation, N.N. and I.Z.H.; formal analysis, N.N. and I.Z.H.; investigation, N.N and I.Z.H.; resources, R.K.C. and R.K.; data curation, N.N.; writing—original draft preparation, N.N.; writing—review and editing, N.N. and I.Z.H.; visualization, N.N. and R.K.C.; supervision, I.Z.H.; project administration, I.Z.H. and N.N. All authors have read and agreed to the published version of the manuscript.

Funding: This work was supported in part by the Critical Materials Innovation Hub, funded by the US Department of Energy, Office of Energy Efficiency and Renewable Energy, Advanced Materials and Manufacturing Technologies Office, DOE grant number AL-12-350-001. Ames National Laboratory is operated for the U.S. DOE by Iowa State University under contract number DE-AC02-07CH11358.

Data Availability Statement: All data is available from the references cited.

Acknowledgments: The authors would like to pay tribute to their supervisor, the late Vitalij Pecharsky, whose enduring influence and commitment to group members serve as a source of inspiration.

Conflicts of Interest: The authors declare no conflicts of interest.

References

1. Hart, W.A.; Beumel, O.; Whaley, T.P. *The chemistry of Lithium. Sodium, Potassium, Rubidium, Cesium and Francium*; Pergmum Press: New York, NY, USA; Oxford, UK, 1973; Volume 13.
2. Christmann, P.; Gloaguen, E.; Labbé, J.-F.; Melleton, J.; Piantone, P. Global lithium resources and sustainability issues. In *Lithium Process Chemistry*; Elsevier: Amsterdam, The Netherlands, 2015; pp. 1–40.
3. Nandihalli, N. A Review of Nanocarbon-Based Anode Materials for Lithium-Ion Batteries. *Crystals* **2024**, *14*, 800. [CrossRef]
4. Gao, Z.; Xie, H.; Yang, X.; Zhang, L.; Yu, H.; Wang, W.; Liu, Y.; Xu, Y.; Ma, B.; Liu, X. Electric vehicle lifecycle carbon emission reduction: A review. *Carbon Neutralization* **2023**, *2*, 528–550. [CrossRef]
5. Demin, S.V.; Zhilov, V.I.; Tsivadze, A. Lithium and boron isotope effects in extraction systems. *Russ. J. Inorg. Chem.* **2015**, *60*, 633–637. [CrossRef]

6. Sheng, B.; Su, H.; Yu, J.; Lin, S. Lithium extraction process from low grade Na^+/K^+ brines dependent on high layer charge layered double hydroxides. *Desalination* **2023**, *565*, 116856. [CrossRef]
7. Kamienski, C.W.; McDonald, D.P.; Stark, M.W.; Papcun, J.R. Lithium and lithium compounds. In *Kirk-Othmer Encyclopedia of Chemical Technology*; Wiley: Hoboken, NJ, USA, 2000.
8. Tran, T.; Luong, V.T. Lithium production processes. In *Lithium Process Chemistry*; Elsevier: Amsterdam, The Netherlands, 2015; pp. 81–124.
9. Vera, M.L.; Torres, W.R.; Galli, C.I.; Chagnes, A.; Flexer, V. Environmental impact of direct lithium extraction from brines. *Nat. Rev. Earth Environ.* **2023**, *4*, 149–165. [CrossRef]
10. Ash, S. *Mineral Commodity Summaries 2019*; US Geological Survey: Reston, VA, USA, 2019.
11. Rosales, G.D.; del Carmen Ruiz, M.; Rodriguez, M.H. Novel process for the extraction of lithium from β-spodumene by leaching with HF. *Hydrometallurgy* **2014**, *147*, 1–6. [CrossRef]
12. Meshram, P.; Pandey, B.D.; Mankhand, T.R. Extraction of lithium from primary and secondary sources by pre-treatment, leaching and separation: A comprehensive review. *Hydrometallurgy* **2014**, *150*, 192–208. [CrossRef]
13. Garrett, D.E. *Handbook of Lithium and Natural Calcium Chloride: Their Deposits, Processing, Uses and Properties*, 1st ed.; Elsevier: Amsterdam, The Netherlands, 2004.
14. Labbé, J.-F.; Daw, G. Panorama 2011 du Marché du Lithium. Bureau de Recherches Géologiques et Minières [BRGM]; Centre d'Economie de la Sorbonne [CES]. 2012. Available online: https://shs.hal.science/halshs-00809298/ (accessed on 26 September 2024).
15. Li, C.-T.; Peacor, D.R. The crystal structure of $LiAlSi_2O_6$-II ("β spodumene"). *Z. Für Krist.-Cryst. Mater.* **1968**, *126*, 46–65. [CrossRef]
16. Peltosaari, O.; Tanskanen, P.; Heikkinen, E.P.; Fabritius, T. α→ γ→ β-phase transformation of spodumene with hybrid microwave and conventional furnaces. *Miner. Eng.* **2015**, *82*, 54–60. [CrossRef]
17. Salakjani, N.K.; Singh, P.; Nikoloski, A.N. Production of lithium–A literature review. Part 2. Extraction from spodumene. *Miner. Process. Extr. Metall. Rev.* **2019**, *42*, 268–283. [CrossRef]
18. Fasshauer, D.W.; Chatterjee, N.D.; Cemic, L. A thermodynamic analysis of the system $LiAlSiO_4$-$NaAlSiO_4$-Al_2O_3-SiO_2-H_2O based on new heat capacity, thermal expansion, and compressibility data for selected phases. *Contrib. Mineral. Petrol.* **1998**, *133*, 186–198. [CrossRef]
19. Choubey, P.K.; Kim, M.S.; Srivastava, R.R.; Lee, J.-c.; Lee, J.Y. Advance review on the exploitation of the prominent energy-storage element: Lithium. Part I: From mineral and brine resources. *Miner. Eng.* **2016**, *89*, 119–137. [CrossRef]
20. Barbosa, L.I.; Valente, G.; Orosco, R.P.; Gonzalez, J.A. Lithium extraction from β-spodumene through chlorination with chlorine gas. *Miner. Eng.* **2014**, *56*, 29–34. [CrossRef]
21. Li, H.; Eksteen, J.; Kuang, G. Recovery of lithium from mineral resources: State-of-the-art and perspectives–A review. *Hydrometallurgy* **2019**, *189*, 105129. [CrossRef]
22. Karrech, A.; Azadi, M.R.; Elchalakani, M.; Shahin, M.A.; Seibi, A.C. A review on methods for liberating lithium from pegmatities. *Miner. Eng.* **2020**, *145*, 106085. [CrossRef]
23. Dessemond, C.; Soucy, G.; Harvey, J.-P.; Ouzilleau, P. Phase Transitions in the α–γ–β Spodumene Thermodynamic System and Impact of γ-Spodumene on the Efficiency of Lithium Extraction by Acid Leaching. *Minerals* **2020**, *10*, 519. [CrossRef]
24. Peltosaari, O.; Tanskanen, P.; Hautala, S.; Heikkinen, E.P.; Fabritius, T. Mechanical enrichment of converted spodumene by selective sieving. *Miner. Eng.* **2016**, *98*, 30–39. [CrossRef]
25. Kaunda, R.B. Potential environmental impacts of lithium mining. *J. Energy Nat. Resour. Law* **2020**, *38*, 237–244. [CrossRef]
26. Graham, J.D.; Rupp, J.A.; Brungard, E. Lithium in the green energy transition: The quest for both sustainability and security. *Sustainability* **2021**, *13*, 11274. [CrossRef]
27. Hu, Z.; Gao, S.; Liu, Y.; Hu, S.; Zhao, L.; Li, Y.; Wang, Q. NH 4 F assisted high pressure digestion of geological samples for multi-element analysis by ICP-MS. *J. Anal. At. Spectrom.* **2010**, *25*, 408–413. [CrossRef]
28. Zhang, W.; Hu, Z. Recent advances in sample preparation methods for elemental and isotopic analysis of geological samples. *Spectrochim. Acta Part B At. Spectrosc.* **2019**, *160*, 105690. [CrossRef]
29. Richter, R.C.; Nóbrega, J.A.; Pirola, C. *Think Blank: Clean Chemistry Tools for Atomic Spectroscopy*; IKONOS srl: Rome, Italy, 2016.
30. Mariet, C.; Belhadj, O.; Leroy, S.; Carrot, F.; Métrich, N. Relevance of NH_4F in acid digestion before ICP-MS analysis. *Talanta* **2008**, *77*, 445–450. [CrossRef] [PubMed]
31. Zhang, N.; Gao, X.; Shen, Y.; Wang, C.; Wang, J. Effects of ammonium fluoride on the decomposition of geochemical samples as fluorinating agent and its analytical application. *Anal. Sci.* **2013**, *29*, 441–446. [CrossRef] [PubMed]
32. Ammann, A.A. Inductively coupled plasma mass spectrometry (ICP MS): A versatile tool. *J. Mass Spectrom.* **2007**, *42*, 419–427. [CrossRef]
33. Freiser, H. *Ion-Selective Electrodes in Analytical Chemistry*; Springer Science & Business Media: Berlin/Heidelberg, Germany, 2012.
34. Murphy, K.R.; Stedmon, C.A.; Graeber, D.; Bro, R. Fluorescence spectroscopy and multi-way techniques. PARAFAC. *Anal. Methods* **2013**, *5*, 6557–6566. [CrossRef]
35. Chauhan, A.; Chauhan, P. Powder XRD technique and its applications in science and technology. *J. Anal. Bioanal. Tech.* **2014**, *5*, 5. [CrossRef]

36. Wilde, A.; Otto, A.; McCracken, S. Geology of the Goulamina spodumene pegmatite field, Mali. *Ore Geol. Rev.* **2021**, *134*, 104162. [CrossRef]
37. Volpi, M.; Pirola, C.; Rota, G.; Nóbrega, J.A.; Carnaroglio, D. Microwave-assisted sample preparation of α-spodumene: A simple procedure for analysis of a complex sample. *Miner. Eng.* **2022**, *187*, 107820. [CrossRef]
38. Bale, M.D.; May, A.V. Processing of ores to produce tantalum and lithium. *Miner. Eng.* **1989**, *2*, 299–320. [CrossRef]
39. Amarante, M.; De Sousa, A.B.; Leite, M.M. Processing a spodumene ore to obtain lithium concentrates for addition to glass and ceramic bodies. *Miner. Eng.* **1999**, *12*, 433–436. [CrossRef]
40. Li, Y.; Cheng, G.; Zhang, M.; Cao, Y.; Von Lau, E. Advances in depressants used for pyrite flotation separation from coal/minerals. *Int. J. Coal Sci. Technol.* **2022**, *9*, 54. [CrossRef]
41. Tadesse, B.; Makuei, F.; Albijanic, B.; Dyer, L. The beneficiation of lithium minerals from hard rock ores: A review. *Miner. Eng.* **2019**, *131*, 170–184. [CrossRef]
42. Cheng, G.; Xiong, L.; Lu, Y.; Zhang, Z.G.; Lv, C.; Lau, E.V. Advancements in the application of surface roughness in mineral flotation process. *Sep. Sci. Technol.* **2024**, *59*, 592–611. [CrossRef]
43. Mingshun, X.; Shiheng, W.; Qinfang, Z. Leaching mechanism of the spodumene sulphuric acid process. *Rare Met. (Engl. Ed.)* **1997**, *16*, 36–44.
44. Tian, Q.; Chen, B.; Chen, Y.; Ma, L.; Shi, X. Roasting and leaching behavior of spodumene in sulphuric acid process. *Xiyou Jinshu/Chin. J. Rare Met.* **2011**, *35*, 118–123.
45. Kuang, G.; Chen, Z.B.; Guo, H.; Li, M.H. Lithium extraction mechanism from α-spodumene by fluorine chemical method. *Adv. Mater. Res.* **2012**, *524*, 2011–2016. [CrossRef]
46. Rosales, G.D.; del Carmen Ruiz, M.; Rodriguez, M.H. Alkaline metal fluoride synthesis as a subproduct of β-spodumene leaching. *Hydrometallurgy* **2013**, *139*, 73–78. [CrossRef]
47. Guo, H.; Kuang, G.; Wang, H.; Yu, H.; Zhao, X. Investigation of enhanced leaching of lithium from α-spodumene using hydrofluoric and sulfuric acid. *Minerals* **2017**, *7*, 205. [CrossRef]
48. Hunwick, R. Recovery of Lithium from Silicate Minerals. U.S. Patent US2017017522, 12 December 2016.
49. Sharma, Y. *Processing of Lithium Containing Ore*; 2014. Available online: https://patents.google.com/patent/US20150152523A1/en (accessed on 26 September 2024).
50. Margarido, F.; Vieceli, N.; Durão, F.; Guimarães, C.; Nogueira, C. Minero-metallurgical processes for lithium recovery from pegmatitic ores= Processos minero-metalúrgicos para a recuperação de lítio de minérios pegmatíticos. *Comun. Geológicas* **2014**, *101*, 795–798.
51. Fosu, A.Y.; Kanari, N.; Bartier, D.; Vaughan, J.; Chagnes, A. Novel extraction route of lithium from α-spodumene by dry chlorination. *RSC Adv.* **2022**, *12*, 21468–21481. [CrossRef]
52. Jena, P.K.; Brocchi, E.A. Metal extraction through chlorine metallurgy. *Miner. Process. Extr. Metall. Rev.* **1997**, *16*, 211–237. [CrossRef]
53. Liu, J.; Wen, S.-m.; Chen, Y.; Liu, D.; Bai, S.-j.; Wu, D.-d. Process optimization and reaction mechanism of removing copper from an Fe-rich pyrite cinder using chlorination roasting. *J. Iron. Steel Res. Int.* **2013**, *20*, 20–26. [CrossRef]
54. Barbosa, L.I.; González, J.A.; del Carmen Ruiz, M. Extraction of lithium from β-spodumene using chlorination roasting with calcium chloride. *Thermochim. Acta* **2015**, *605*, 63–67. [CrossRef]
55. Gabra, G.G.; Torma, A.E.; Olivier, C.A. Pressure leaching of beta-spodumene by sodium chloride. *Can. Metall. Q.* **1975**, *14*, 355–359. [CrossRef]
56. Medina, L.F.; El-Naggar, M. An alternative method for the recovery of lithium from spodumene. *Metall. Trans. B* **1984**, *15*, 4. [CrossRef]
57. Chen, Y.; Tian, Q.; Chen, B.; Shi, X.; Liao, T. Preparation of lithium carbonate from spodumene by a sodium carbonate autoclave process. *Hydrometallurgy* **2011**, *109*, 43–46. [CrossRef]
58. Tiihonen, M.; Haavanlammi, L.; Kinnunen, S.; Kolehmainen, E. Outotec lithium hydroxide process-a novel direct leach process for the production of battery grade lithium hydroxide monohydrate form calcined spodumene. In Proceedings of the ALTA 2019, Sydney, Australia, 4–6 December 2019; ALTA Metallurgical Services: Perth, Australia, 2019.
59. Zhou, H.; Cao, Z.; Ma, B.; Wang, C.; Chen, Y. Selective and efficient extraction of lithium from spodumene via nitric acid pressure leaching. *Chem. Eng. Sci.* **2024**, *287*, 119736. [CrossRef]
60. Wang, S.; Szymanski, N.J.; Fei, Y.; Dong, W.; Christensen, J.N.; Zeng, Y.; Whittaker, M.; Ceder, G. Direct Lithium Extraction from α-Spodumene through Solid-State Reactions for Sustainable Li_2CO_3 Production. *Inorg. Chem.* **2024**, *63*, 13576–13584. [CrossRef]
61. Xing, P.; Wang, C.; Zeng, L.; Ma, B.; Wang, L.; Chen, Y.; Yang, C. Lithium extraction and hydroxysodalite zeolite synthesis by hydrothermal conversion of α-spodumene. *ACS Sustain. Chem. Eng.* **2019**, *7*, 9498–9505. [CrossRef]
62. Qiu, S.; Liu, C.; Yu, J. Conversion from α-spodumene to intermediate product Li_2SiO_3 by hydrothermal alkaline treatment in the lithium extraction process. *Miner. Eng.* **2022**, *183*, 107599. [CrossRef]
63. Qiu, S.; Zhu, Y.; Jiang, Y.; Liu, C.; Yu, J. Kinetics and Mechanism of Lithium Extraction from α-Spodumene in Potassium Hydroxide Solution. *Ind. Eng. Chem. Res.* **2022**, *61*, 15103–15113. [CrossRef]
64. Song, Y.; Zhao, T.; He, L.; Zhao, Z.; Liu, X. A promising approach for directly extracting lithium from α-spodumene by alkaline digestion and precipitation as phosphate. *Hydrometallurgy* **2019**, *189*, 105141. [CrossRef]

65. Han, S.; Sagzhanov, D.; Pan, J.; Vaziri Hassas, B.; Rezaee, M.; Akbari, H.; Mensah-Biney, R. Direct Extraction of Lithium from α-Spodumene by Salt Roasting–Leaching Process. *ACS Sustain. Chem. Eng.* **2022**, *10*, 13495–13504. [CrossRef]
66. Zhou, H.; Liu, Y.; Ma, B.; Wang, C.; Chen, Y. Strengthening extraction of lithium and rubidium from activated α-spodumene concentrate via sodium carbonate roasting. *J. Ind. Eng. Chem.* **2023**, *123*, 248–259. [CrossRef]
67. Braga, P.; França, S.; Neumann, R.; Rodriguez, M.; Rosales, G. Alkaline process for extracting lithium from Spodumene. In Proceedings of the 11th International Seminar on Process Hydrometallurgy-Hydroprocess, Santiago, Chile, 19–21 June 2019; pp. 19–21.
68. Maurice, A.; Olivier, C.A. Carbonatizing Roast of Lithiumbearing Ores. U.S. Patent US3380802A, 30 April 1968.
69. McIntosh, N.C. Production of Lithium Compounds. U.S. Patent US2413644A, 27 February 1943.
70. Zhang, Y.; Ma, B.; Lv, Y.; Wang, C.; Chen, Y. An effective method for directly extracting lithium from α-spodumene by activated roasting and sulfuric acid leaching. *J. Ind. Eng. Chem.* **2023**, *122*, 540–550. [CrossRef]
71. Lee, D.; Joo, Y.-Y.; Shin, D.J.; Shin, S.M. Recovery of Lithium from Beta-Spodumene Through Serial Calcination and Water Leaching with CaO. *JOM* **2024**, *76*, 1477–1484. [CrossRef]
72. Zelikman, A.N.; Krein, O.E.; Samsonov, G.V. *Metallurgy of Rare Metals*; Isreal Program for Scientific Translations: Jarusalem, Isreal, 1966.
73. Kuang, G.; Liu, Y.; Li, H.; Xing, S.; Li, F.; Guo, H. Extraction of lithium from β-spodumene using sodium sulfate solution. *Hydrometallurgy* **2018**, *177*, 49–56. [CrossRef]
74. Ncube, T.; Oskierski, H.; Senanayake, G.; Dlugogorski, B.Z. Two-step reaction mechanism of roasting spodumene with potassium sulfate. *Inorg. Chem.* **2021**, *60*, 3620–3625. [CrossRef]
75. Suharyanto, A.; Lalasari, L.H.; Mubarok, M.Z. Decomposition of spodumene mineral in granitic rocks from South Kalimantan-Indonesia by potassium sulphate. In *IOP Conference Series: Materials Science and Engineering*; IOP Publishing: Bristol, UK, 2019; p. 012044.
76. Laferrière, A.; Dessureault, Y.; Skiadas, N.; Gary, H.K.; Pearse, A.L. *NI 43-101 Technical Report: Preliminary Economic Assessment of the Whabouchi Lithium Deposit and Hydromet Plant*; Nemaska Lithium Inc.: Montreal, AC, Canada, 2012.
77. Archarnhault, M.Q.; Quebec, A.O.C. Carbonatizing Roast of Lithium Bearing Ores. U.S. Patent 3380802, 30 April 1968.
78. Peterson, J.A.; Gloss, G.H. Lithium Values Recovery Process. U.S. Patent 2893828, 7 July 1959.
79. Erasmus, H.D.W. Method of Treating Lithiferous Ores to Recover Lithium as Lithium Chloride. U.S. Patent 2561439, 24 July 1951.
80. Zelikman, A.N.; Krein, O.E.; Sansonov, G.V. *Metallurgy of Rare Metals ((Translated from Russian) 458*; NASA and National Science Foundation: Washington, DC, USA, 1966.
81. Victor, K.A. Method of Recovering Lithium Compounds from Lithium Minerals. US Patent 2662809, 15 December 1953.
82. Hayes, E.T.; Williams, F.P.; Sternberg, W.M. Production of Lithium Chloride from Spodumene. U.S. Patent 2533246, 12 December 1950.
83. Rosales, G.D.; Resentera, A.C.; Gonzalez, J.A.; Wuilloud, R.G.; Rodriguez, M.H. Efficient extraction of lithium from β-spodumene by direct roasting with NaF and leaching. *Chem. Eng. Res. Des.* **2019**, *150*, 320–326. [CrossRef]
84. Hui, G.; Yu, H.z.; Zhou, A.; LÜ, M.H.; Qiao, W.; Kuang, G.; Wang, H.D. Kinetics of leaching lithium from α-spodumene in enhanced acid treatment using HF/H_2SO_4 as medium. *Trans. Nonferrous Met. Soc. China* **2019**, *29*, 407–415. [CrossRef]
85. Mishra, R.R.; Sharma, A.K. Microwave–material interaction phenomena: Heating mechanisms, challenges and opportunities in material processing. *Compos. Part A* **2016**, *81*, 78–97. [CrossRef]
86. Mishra, R.R.; Sharma, A.K. A review of research trends in microwave processing of metal-based materials and opportunities in microwave metal casting. *Crit. Rev. Solid State Mater. Sci.* **2016**, *41*, 217–255. [CrossRef]
87. Nandihalli, N.; Gregory, D.H.; Mori, T. Energy-Saving Pathways for Thermoelectric Nanomaterial Synthesis: Hydrothermal/Solvothermal, Microwave-Assisted, Solution-Based, and Powder Processing. *Adv. Sci.* **2022**, *9*, 2106052. [CrossRef]
88. Rao, K.J.; Vaidhyanathan, B.; Ganguli, M.; Ramakrishnan, P.A. Synthesis of inorganic solids using microwaves. *Chem. Mater.* **1999**, *11*, 882–895. [CrossRef]
89. Antonucci, V.; Correa, C. Sulfuric Acid Leaching of Chalcopyrite Concentrate Assisted by Application of Microwave Energy, Paper from COPPER 95, Volume III, Electrorefining and Hydrometallurgy of Copper. In Proceedings of the International Conference, Santiago, Chile, 26–29 November 1995; pp. 549–557.
90. Beard, G.; Belcher, W.; Bradhurst, D.; Worner, H.; Cook, J. Microwave-Assisted Smelting of Rare-Earth Magnet Alloys. In Proceedings of the Twelfth International Workshop on Rare-Earth Magnets and Their Applications, Canberra, Australia, 12–15 July 1992; pp. 665–669.
91. Yixin, L.C.X.Y.H. Application of microwave radiation to extractive metallurgy. *J. Mater. Sci. Technol.* **1990**, *6*, 121.
92. Gomez, I.; Aguilar, J.A. Microwaves for reduction of iron ore pellet by carbon. *MRS Online Proc. Libr.* **1994**, *366*, 347. [CrossRef]
93. Salakjani, N.K.; Nikoloski, A.N.; Singh, P. Mineralogical transformations of spodumene concentrate from Greenbushes, Western Australia. Part 2: Microwave heating. *Miner. Eng.* **2017**, *100*, 191–199. [CrossRef]
94. Salakjani, N.K.; Singh, P.; Nikoloski, A.N. Acid roasting of spodumene: Microwave vs. conventional heating. *Miner. Eng.* **2019**, *138*, 161–167. [CrossRef]
95. Rezaee, M.; Han, S.; Sagzhanov, D.; Hassas, B.V.; Slawecki, T.M.; Agrawal, D.; Akbari, H.; Mensah-Biney, R. Microwave-assisted calcination of spodumene for efficient, low-cost and environmentally friendly extraction of lithium. *Powder Technol.* **2022**, *397*, 116992. [CrossRef]

96. Krivolapova, O.N.; Fureev, I.L. Application of microwave radiation for decrepitation of spodumene from the Kolmozerskoe deposit. *Non-Ferr. Metall.* **2023**, *29*, 5–12. [CrossRef]
97. Luong, V.T.; Kang, D.J.; An, J.W.; Kim, M.J.; Tran, T. Factors affecting the extraction of lithium from lepidolite. *Hydrometallurgy* **2013**, *134*, 54–61. [CrossRef]
98. Alex, T.C.; Kumar, R.; Roy, S.K.; Mehrotra, S.P. Mechanical activation of Al-oxyhydroxide minerals–A review. *Miner. Process. Extr. Metall. Rev.* **2016**, *37*, 1–26. [CrossRef]
99. Kotsupalo, N.P.; Menzheres, L.T.; Ryabtsev, A.D.; Boldyrev, V.V. Mechanical activation of α-spodumene for further processing into lithium compounds. *Theor. Found. Chem. Eng.* **2010**, *44*, 503–507. [CrossRef]
100. Necke, T.; Stein, J.; Kleebe, H.-J.; Balke-Grünewald, B. Lithium Extraction and Zeolite Synthesis via Mechanochemical Treatment of the Silicate Minerals Lepidolite, Spodumene, and Petalite. *Minerals* **2023**, *13*, 1030. [CrossRef]
101. Gasalla, H.J.; Aglietti, E.F.; Lopez, J.M.P.; Pereira, E. Changes in physicochemical properties of α-spodumene by mechanochemical treatment. *Mater. Chem. Phys.* **1987**, *17*, 379–389. [CrossRef]
102. Berger, A.; Boldyrev, V.; Menzheres, L. Mechanical activation of β-spodumene. *Mater. Chem. Phys.* **1990**, *25*, 339–350. [CrossRef]
103. Rosales, G.D.; Resentera, A.C.J.; Wuilloud, R.G.; Rodriguez, M.H.; Esquivel, M.R. Optimization of combined mechanical activation-leaching parameters of low-grade α-spodumene/NaF mixture using response surface methodology. *Miner. Eng.* **2022**, *184*, 107633. [CrossRef]
104. Dobó, Z.; Dinh, T.; Kulcsár, T. A review on recycling of spent lithium-ion batteries. *Energy Rep.* **2023**, *9*, 6362–6395. [CrossRef]
105. Tawonezvi, T.; Nomnqa, M.; Petrik, L.; Bladergroen, B.J. Recovery and recycling of valuable metals from spent lithium-ion batteries: A comprehensive review and analysis. *Energies* **2023**, *16*, 1365. [CrossRef]
106. Krishnan, R.; Gopan, G. A Comprehensive Review of Lithium Extraction: From Historical Perspectives to Emerging Technologies, Storage, and Environmental Considerations. *Cleaner Eng. Technol.* **2024**, *20*, 100749. [CrossRef]
107. Ren, L.; Liu, B.; Bao, S.; Ding, W.; Zhang, Y.; Hou, X.; Lin, C.; Chen, B. Recovery of Li, Ni, Co and Mn from spent lithium-ion batteries assisted by organic acids: Process optimization and leaching mechanism. *Int. J. Miner. Metall. Mater.* **2024**, *31*, 518–530. [CrossRef]
108. Yao, Y.; Zhu, M.; Zhao, Z.; Tong, B.; Fan, Y.; Hua, Z. Hydrometallurgical processes for recycling spent lithium-ion batteries: A critical review. *ACS Sustain. Chem. Eng.* **2018**, *6*, 13611–13627. [CrossRef]
109. Peng, Q.; Zhu, X.; Li, J.; Liao, Q.; Lai, Y.; Zhang, L.; Fu, Q.; Zhu, X. A novel method for carbon removal and valuable metal recovery by incorporating steam into the reduction-roasting process of spent lithium-ion batteries. *Waste Manag.* **2021**, *134*, 100–109. [CrossRef]
110. Yang, C.; Zhang, J.; Yu, B.; Huang, H.; Chen, Y.; Wang, C. Recovery of valuable metals from spent $LiNi_xCo_yMnZO_2$ cathode material via phase transformation and stepwise leaching. *Sep. Purif. Technol.* **2021**, *267*, 118609. [CrossRef]
111. Lin, J.; Li, L.; Fan, E.; Liu, C.; Zhang, X.; Cao, H.; Sun, Z.; Chen, R. Conversion mechanisms of selective extraction of lithium from spent lithium-ion batteries by sulfation roasting. *ACS Appl. Mater. Interfaces* **2020**, *12*, 18482–18489. [CrossRef]
112. Makuza, B.; Yu, D.; Huang, Z.; Tian, Q.; Guo, X. Dry grinding-carbonated ultrasound-assisted water leaching of carbothermally reduced lithium-ion battery black mass towards enhanced selective extraction of lithium and recovery of high-value metals. *Resour. Conserv. Recycl.* **2021**, *174*, 105784. [CrossRef]
113. Pinegar, H.; Smith, Y.R. Recycling of end-of-life lithium ion batteries, Part I: Commercial processes. *J. Sustain. Metall.* **2019**, *5*, 402–416. [CrossRef]
114. Ding, W.; Bao, S.; Zhang, Y.; Ren, L.; Xin, C.; Chen, B.; Liu, B.; Xiao, J.; Hou, X. Stepwise recycling of valuable metals from spent lithium-ion batteries based on in situ thermal reduction and ultrasonic-assisted water leaching. *Green Chem.* **2023**, *25*, 6652–6665. [CrossRef]
115. Takacova, Z.; Orac, D.; Klimko, J.; Miskufova, A. Current trends in spent portable lithium battery recycling. *Materials* **2023**, *16*, 4264. [CrossRef] [PubMed]
116. Chen, W.-S.; Ho, H.-J. Recovery of valuable metals from lithium-ion batteries NMC cathode waste materials by hydrometallurgical methods. *Metals* **2018**, *8*, 321. [CrossRef]
117. Zhang, G.; Du, Z.; He, Y.; Wang, H.; Xie, W.; Zhang, T. A sustainable process for the recovery of anode and cathode materials derived from spent lithium-ion batteries. *Sustainability* **2019**, *11*, 2363. [CrossRef]
118. Klimko, J.; Oráč, D.; Miškufová, A.; Vonderstein, C.; Dertmann, C.; Sommerfeld, M.; Friedrich, B.; Havlík, T. A combined pyro-and hydrometallurgical approach to recycle pyrolyzed lithium-ion battery black mass part 2: Lithium recovery from Li enriched slag—Thermodynamic study, kinetic study, and dry digestion. *Metals* **2020**, *10*, 1558. [CrossRef]
119. Peng, C.; Liu, F.; Aji, A.T.; Wilson, B.P.; Lundström, M. Extraction of Li and Co from industrially produced Li-ion battery waste–Using the reductive power of waste itself. *Waste Manag.* **2019**, *95*, 604–611. [CrossRef] [PubMed]
120. Chen, X.; Cao, L.; Kang, D.; Li, J.; Zhou, T.; Ma, H. Recovery of valuable metals from mixed types of spent lithium ion batteries. Part II: Selective extraction of lithium. *Waste Manag.* **2018**, *80*, 198–210. [CrossRef] [PubMed]
121. Tang, Y.C.; Wang, J.Z.; Shen, Y.H. Separation of valuable metals in the recycling of lithium batteries via solvent extraction. *Minerals* **2023**, *13*, 285. [CrossRef]
122. Garcia, L.V.; Ho, Y.-C.; Myo Thant, M.M.; Han, D.S.; Lim, J.W. Lithium in a sustainable circular economy: A comprehensive review. *Processes* **2023**, *11*, 418. [CrossRef]

123. Zanoletti, A.; Carena, E.; Ferrara, C.; Bontempi, E. A Review of Lithium-Ion Battery Recycling: Technologies, Sustainability, and Open Issues. *Batteries* **2024**, *10*, 38. [CrossRef]
124. Gerold, E.; Luidold, S.; Antrekowitsch, H. Separation and efficient recovery of lithium from spent lithium-ion batteries. *Metals* **2021**, *11*, 1091. [CrossRef]
125. Marchese, D.; Giosuè, C.; Staffolani, A.; Conti, M.; Orcioni, S.; Soavi, F.; Cavalletti, M.; Stipa, P. An overview of the sustainable recycling processes used for lithium-ion batteries. *Batteries* **2024**, *10*, 27. [CrossRef]
126. Rautela, R.; Yadav, B.R.; Kumar, S. A review on technologies for recovery of metals from waste lithium-ion batteries. *J. Power Sources* **2023**, *580*, 233428. [CrossRef]
127. Tiihonen, M. Method of Extracting Lithium Compound (s). U.S. Patent US20210147247A1, 20 May 2021.
128. Tiihonen, M.; Haavanlammi, L. Method for Recovering Lithium Carbonate. U.S. Patent US9255012B2, 9 February 2016.
129. Kiggins, C.; Cook, J.; Ates, M.N.; Busbee, J.; Lee, B. Methods for Extracting Lithium from Spodumene. U.S. Patent US20200399772A1, 24 December 2020.
130. Haynes, B.; Mann, J. Apparatus for Extracting Lithium from Ore. U.S. Patent US20240102126A1, 28 March 2024.
131. Anovitz, L.; Blencoe, J.; Palmer, D. Method of Extracting Lithium. U.S. Patent US20060171869A1, 3 August 2006.
132. Di Cesare, E. Method of Mineral Recovery. U.S. Patent EP3911772A1, 24 March 2022.
133. Ellestad, R.B.; Milne, L.K. Method of Extracting Lithium Values from Spodumene Ores. U.S. Patent US2516109A, 25 July 1950.
134. Sun, Z.; Chen, H.; Caldwell, T.B.; Thurston, A.M. Selective Extraction of Lithium from Clay Minerals. U.S. Patent US20210207243A1, 8 July 2021.
135. Dunn, W.E., Jr.; Van Jahnke, J. Cyclical Vacuum Chlorination Processes, including Lithium Extraction. U.S. Patent US7588741B2, 15 September 2009.
136. Blencoe, J.G.; Groen, A. Process for Extracting Lithium, Aluminum, and Silicon Materials from a Hard Rock Source. U.S. Patent US20240132991A1, 25 April 2024.
137. Rodriguez, M.H.; Beiza, A.C.R.; Rosales, G.D. Pyrometallurgical Method for Obtaining Compounds of Lithium and Intermediates from Alpha-Spodumene and Lepidolite. U.S. Patent US20200325557A1, 13 June 2023.
138. Sharma, Y. Processing of Lithium Containing Material including HCl Sparge. U.S. Patent WO2016119003A1, 29 March 2022.
139. Swonger, L.R. Producing Lithium. U.S. Patent US20150014184A1, 15 January 2015.
140. Magnan, J.-F.; Bourassa, G.; Laroche, N.; Pearse, G.; Mackie, S.C.; Gladkovas, M.; Symons, P.; Genders, J.D.; Clayton, G.; Bouchard, P. Methods for Treating Lithium-Containing Materials. U.S. Patent US20210363648A1, 6 December 2022.
141. Amouzegar, K.; Amant, G.S.; Harrison, S. Process for the Purification of Lithium Carbonate. U.S. Patent US6048507A, 11 April 2000.
142. Catovic, E. Process for Extracting and Recovering Lithium Values from Lithium Bearing Materials. U.S. Patent US20190048438A1, 5 January 2021.
143. Oetzel, E.; Kräuter, R. Method for Producing Solid Particles, Solid Particles, and the Use Thereof. CN Patent CN113454249A, 24 February 2022.
144. Qingsheng, W. Method for Greatly Reducing Sulphate Content in Various Levels of Lithium Carbonate in Spodumene Sulfuric Acid Method. U.S. Patent US20210309534A1, 7 October 2021.
145. Haynes, B.; Mann, J. Lithium Extraction Method. U.S. Patent US11371116B2, 28 June 2022.

Disclaimer/Publisher's Note: The statements, opinions and data contained in all publications are solely those of the individual author(s) and contributor(s) and not of MDPI and/or the editor(s). MDPI and/or the editor(s) disclaim responsibility for any injury to people or property resulting from any ideas, methods, instructions or products referred to in the content.